Chemistry and Physics of Lipids xxx (2014) xxx–xxx

Contents lists available at ScienceDirect

Chemistry and Physics of Lipids

journal homepage: www.elsevier.com/locate/chemphyslip

Novel cationic polyene glycol phospholipids as DNA transfer reagents—Lack of a structure–activity relationship due to uncontrolled self-assembling processes

Christer L. Øpstad[a], Muhammad Zeeshan[a], Asma Zaidi[a], Hans-Richard Sliwka[a,*], Vassilia Partali[a], David G. Nicholson[a], Chinmay Surve[b], Mitchell A. Izower[b], Natalia Bilchuk[b], Howard H. Lou[b], Philip. L. Leopold[b], Helge Larsen[c], Alexandra Liberska[a,d], Nada Abdul Khalique[d], Liji Raju[d], Marcella Flinterman[d], Emile Jubeli[d], Michael D. Pungente[e]

[a] Department of Chemistry, Norwegian University of Science and Technology (NTNU), 7491 Trondheim, Norway
[b] Department of Chemistry, Chemical Biology & Biomedical Engineering, Stevens Institute of Technology, Hoboken, NJ 07030, United States
[c] Department of Physics, University of Stavanger, 4036 Stavanger, Norway
[d] Research Division, Weill Cornell Medical College in Qatar, P.O. Box 24144, Doha, Qatar
[e] Pre-Medical Unit, Weill Cornell Medical College in Qatar, P.O. Box 24144, Doha, Qatar

ARTICLE INFO

Article history:
Received 3 February 2014
Received in revised form 31 March 2014
Accepted 1 April 2014
Available online xxx

Keywords:
Aggregation
Amphiphiles
Carotenoids
Cations
DNA
Lipids

ABSTRACT

Cationic glycol phospholipids were synthesized introducing chromophoric, rigid polyenoic $C_{20:5}$ and $C_{30:9}$ chains next to saturated flexible alkyl chains of variable lengths $C_{6\text{-}20:0}$. Surface properties and liposome formation of the amphiphilic compounds were determined, the properties of liposome/DNA complexes (lipoplexes) were established using three formulations (no co-lipid, DOPE as a co-lipid, or cholesterol as a co-lipid), and the microstructure of the best transfecting compounds inspected using small angle X-ray diffraction to explore details of the partially ordered structures of the systems that constitute the series. Transfection and cytotoxicity of the lipoplexes were evaluated by DNA delivery to Chinese hamster ovary (CHO-K1) cells using the cationic glycerol phospholipid 1,2-dioleoyl-*sn*-glycero-3-ethylphosphocholine (EPC) as a reference compound.

The uncontrollable self-association of the molecules in water resulted in aggregates and liposomes of quite different sizes without a structure–property relationship. Likewise, adding DNA to the liposomes gave rise to unpredictable sized lipoplexes, which, again, transfected without a structure–activity relationship. Nevertheless, one compound among the novel lipids ($C_{30:9}$ chain paired with a $C_{20:0}$ chain) exhibited comparable transfection efficiency and toxicity to the control cationic lipid EPC. Thus, the presence of a rigid polyene chain in this best performing achiral glycol lipid did not have an influence on transfection compared with the chiral glycerolipid reference ethyl phosphocholine EPC with two flexible saturated C_{14} chains.

1. Introduction

Cationic lipids have been used as nucleic acid (NA) carriers to eukaryotic cells for more than 25 years (Felgner et al., 1987). Nevertheless, gene transport with these lipids is still in a trial and error phase, as illustrated in a study wherein 1200 tested compounds revealed that only 65 (5%) delivered NA into cells as well as or better than Lipofectamine (Chu et al., 2009), a commonly applied gene delivery formulation (Goldberg, 2008, p. 35). The various biological and chemical variables have so far prevented establishing an unambiguous structure–activity connection (Koynova and Tenchov, 2010; Zhi et al., 2010, 2013). Even so, about 6% of all clinical gene therapy trials are based on lipoplexes prepared with cationic phospholipids (Ginn et al., 2013). Most glycerolipid gene carriers, including EPC, contain flexible saturated or

* Corresponding author. Tel.: +47 73 59 5600.
E-mail address: richard.sliwka@ntnu.no (H.-R. Sliwka).

http://dx.doi.org/10.1016/j.chemphyslip.2014.04.006
0009-3084/

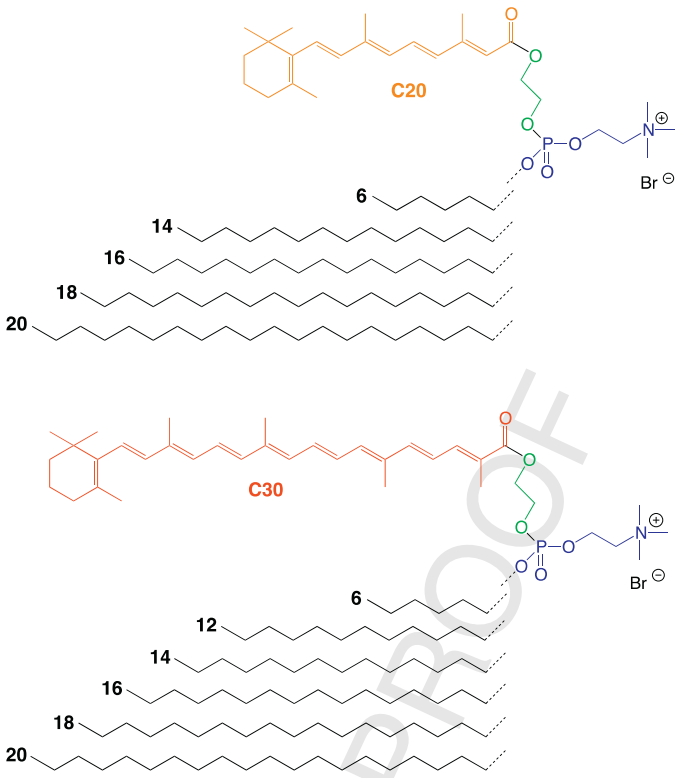

Fig. 1. C20-n and C30-n cationic phosphocholine lipids composed of a "glycol scaffold" (green color), a hydrophobic polyenoic chromophore, either "C20:5" (orange color) or "C30:9" (red color), a hydrophopic alkyl chain and a "hydrophilic head group" (blue color). (For interpretation of the references to color in this figure legend, the reader is referred to the web version of the article.)

mono-unsaturated chains. Rigidity has been introduced with steroids, diphenylethyne and triazine dendrimers (Merkel et al., 2010; Scheule et al., 1998; Zhi et al., 2010). To our knowledge, no precedence for the interplay of polyunsaturated-stiff and saturated-flexible chains in NA carrying phospholipids has yet been specified (Zhi et al., 2010), although this association may be important for adjusting morphology changes along with phase state transitions (cylindrical shape → cone shape = lamellar phase → inverted hexagonal phase) (Adami et al., 2011). Hexagonal phases are either contradictorily considered important or irrelevant for gene transfer (Koynova, 2010). Here, we report on the synthesis of 11 new amphiphilic glycol lipids paired with polyene chains and stepwise increased saturated chains (Fig. 1). The synthesis of the new phospholipids is based on previous connections of polyenes with phosphate groups (Foss et al., 2003, 2004, 2005a,b; Popplewell et al., 2012; Sliwka, 1997, 1999).

A characterization of physical, chemical, and biological properties of the lipids was subsequently performed. The surface properties of these new compounds were compared and their self-assembly into liposomes and to mixed liposomes with (*R*)-1,2-dioleoyl-glycero-3-phosphoethanolamine (DOPE) and (−)-cholesterol (Fig. 2) was examined. EPC, a standard reference cationic lipid (Fig. 2) was included

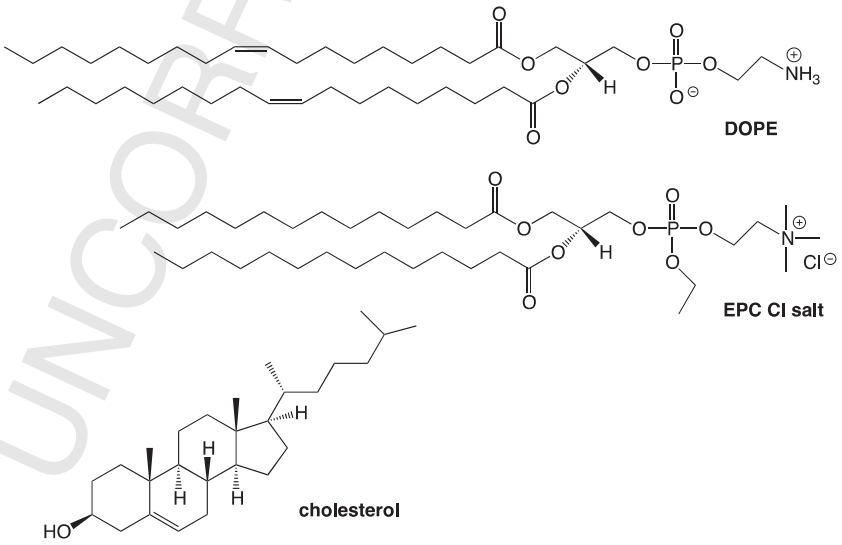

Fig. 2. Structure of dioleoyl ($C_{18:1}$) zwitterionic (*R*)-DOPE, reference dimyristoyl ($C_{14:0}$) cationic (*R*)-EPC and (−)-cholesterol.

Please cite this article in press as: Øpstad, C.L., et al., Novel cationic polyene glycol phospholipids as DNA transfer reagents—Lack of a structure–activity relationship due to uncontrolled self-assembling processes. Chem. Phys. Lipids (2014), http://dx.doi.org/10.1016/j.chemphyslip.2014.04.006

for comparison with the novel polyene cationic lipids. Furthermore, lipoplex formation was assessed following combination of DNA with the liposomes. The size and polydispersity of liposomes and lipoplexes were determined, and the ability of the lipids to deliver a DNA cargo into cells as well as the cytotoxicity of the compounds were measured. Finally, the lipid phase for three of the lipoplexes was resolved using small angle X-ray diffraction. The physical and biological data associated with the novel lipids were compared on the basis of molecular structure, physical properties, DNA-transfection efficiency, and cytotoxicity. This investigation expands previous structure–activity relationship studies varying other constitutional parts of cationic phospholipids (Floch et al., 2000; Kedika and Patri, 2011; Koynova and Tenchov, 2009; Niculescu-Duvaz et al., 2003).

2. Materials and methods

2.1. Materials

Ethyl β-apo-8′-carotenoate and retinoic acid was a generous gift from Dr. H. Ernst, BASF AG, Germany. Control cationic lipid 1,2-dioleoyl-*sn*-glycero-3-ethylphosphocholine (EPC) and neutral co-lipid 1,2-dioleoyl-*sn*-glycero-3-phosphoethanolamine (DOPE) were delivered by Avanti Polar Lipids (Alabaster, AL). Chinese hamster ovary (CHO-K1) cells were obtained from the American Type Culture Collection (ATCC, Manassas, VA, USA). RPMI 1640 medium was purchased from Invitrogen (Grand Island, NY, USA), FBS and antibiotic antimitotic solution containing penicillin, streptomycin and amphotericin B were purchased from Sigma–Aldrich Chemical Co. (St. Louis, MO, USA). Plasmid DNA containing the β-galactosidase gene, pCMVβ*lacZnls12co* was from Marker Gene Technologies, Inc. (Oregon, USA). Cell Titer 96® AQ_{ueous} One Solution Cell Proliferation Assay and Beta Glo® Assay System were purchased from Promega (Madison, WI, USA), β-galactosidase grade VIII enzyme (0.5 mU/ng) from *Escherichia coli* was purchased from Sigma–Aldrich Chemical Co. (St. Louis, MO, USA), DNase I (2000 units/mL) was purchased from New England Biolabs® Inc. (Ipswich, MA) and BCA Protein Quantitation Assay was purchased from Pierce Biotechnology (Thermo Fisher Scientific, Rockford, IL, USA). 10× Tris–Borate EDTA (TBE) powder was purchased from Invitrogen (Grand Island, NY, USA). Unless otherwise stated, all other chemicals were delivered by Sigma–Aldrich Chemical Co. (St. Louis, MO, USA).

2.2. Physical methods

NMR spectra (^{1}H and ^{13}C) were acquired on a Bruker Avance DPX 400 MHz and Bruker Avance 600 MHz with $CDCl_3$ unless otherwise stated. UV–vis spectra were recorded in CH_2Cl_2 using a Single Beam Thermo Spectronic, Helios γ. Mass spectra data were acquired on a MAT 95XL TermoQuest Finnigan mass spectrometer equipped with an electron ionization or electrospray ionization resource. Flash column chromatography (flash-CC) was carried out with silica gel (Woelm Pharma, 60 mesh) or neutral alumina (II–III Brochmann activity, EcoChrom, 100–150 mesh). Surface tension was determined using a Wilhelmy (Pt) plate on a Krüss Tensiometer K100. The aggregation concentration c_{ag} was found by dissolving the compounds in the indicated solvents. H_2O was added in 100 μl amounts and monitored VIS-spectroscopically for aggregate formation. Inversely, the compounds were dispersed in H_2O and organic solvent was added until disruption of the aggregates.

The small angle X-ray diffraction experiments were performed at the European Synchrotron Radiation Facility (ESRF), Grenoble, France, on the bending magnet BM29 BioSAXS beam line. BM29 is equipped with a double multilayer monochromator (energy band pass $\sim 10^{-2}$) and 4 mrad toroidal mirror 1.1 m long. The experimental hutch is equipped with a marble table housing the modular-length flight tube, 2D detector (Pilatus 1M) and a sample handling equipment (automated sample changer). The sample-to-detector distance was 2.8 m. Samples were prepared in 1 mL Eppendorf tubes, and loaded into the 1.8 mm diameter quartz capillary sample cell by the automated sample changer. Data collection was performed in 16-bunch mode at an energy of 12.5 keV with an exposure time of 2 s per frame using the dedicated beam line software BsxCuBE. The small angle X-ray diffraction curves were obtained by integrating and averaging of 20 2D images. Subsequent processing (such as background subtraction and scaling) and analysis were performed using the ATSAS-software package (Konarev et al., 2003) and MATHEMATICA (Mathematica, 2010).

2.3. Biological methods

Preparation of lipid stock solutions. All lipids were initially dissolved in CH_2Cl_2 in round bottom flasks, followed by evaporation of the organic solvent under reduced pressure resulting in thin films. Ethanol was then added to achieve stock solutions of 1 mM. Care was taken to protect the lipids from air and ambient light. All stock solutions were stored in amber vials under an inert atmosphere (N_2 or Ar) and kept at −80 °C.

Liposome preparation. Liposomes from the new cationic lipids as well as EPC were obtained by hydrating thin lipid films. An overall 3:2 molar ratio of total cationic lipid to co-lipid, either DOPE or cholesterol, in ethanolic solutions were prepared separately and evaporated under reduced pressure to generate thin films. The lipid films were hydrated with a known amount of sterile water to give 2 mM final hydrated stock solutions, which were stored overnight at 4 °C. Before use, the hydrated stocks were warmed to 37 °C and sonicated for 30 min.

Preparation of lipoplexes (lipid/DNA complexes). Lipoplexes of concentrations 0.081 mM, 0.243 mM, 0.486 mM, 0.81 mM and 1.62 mM, corresponding to the N/P (+/−) molar charge ratios of 0.5:1, 1.5:1, 3:1, 5.0:1 and 10.0:1, respectively, were prepared from the 2 mM liposome stocks. OPTI-MEM cell culture medium (57.6 μL) and DNA in E-Toxate™ Water, (14.4 μL; 250 ng/μL) were first combined, followed by the addition of an equal volume of corresponding liposome (72 μL) to this and mixed. These lipoplex formulations were incubated at 22 °C for 30 min.

Liposome and lipoplex sizing. The hydrodynamic diameters d_H of liposomes and lipoplexes were measured by dynamic light scattering (DLS, Malvern Zetasizer APS, Malvern, Worcestershire, UK) at 25 °C with a detection angle of 90°.

Gel retardation assays of lipoplexes. To 20 μL of the lipoplexes, 2 μL of the gel loading dye (6×) was added and mixed by pipetting. Eighteen microliters of each sample was then loaded onto a 1% agarose gel impregnated with ethidium bromide and run at 105 V for 1 h in 1× TBE buffer. The migration of DNA complexed with the cationic lipids was impeded in the electric field. The DNA bands were observed using an ultraviolet transilluminator.

Please cite this article in press as: Øpstad, C.L., et al., Novel cationic polyene glycol phospholipids as DNA transfer reagents—Lack of a structure–activity relationship due to uncontrolled self-assembling processes. Chem. Phys. Lipids (2014), http://dx.doi.org/10.1016/j.chemphyslip.2014.04.006

DNase I degradation assays of lipoplexes. The lipoplexes (20 μL) were incubated with DNase I (2 units) at 37 °C for 1 h. After incubation, 5% SDS (4 μL) was added and incubated for a further 30 min, followed by 2 μL of gel loading dye (6×). Each lipoplex sample (18 μL) was then loaded onto a 1% agarose gel impregnated with ethidium bromide and run at 105 V for 1 h in 1× TBE buffer. The *p*DNA bands were observed using an ultraviolet transilluminator.

Cell culture and transfection. CHO-K1 cells were grown in RPMI media supplemented with 10% fetal calf serum and 100 U/mL of penicillin/streptomycin and 0.25 μg/mL amphotericin B. Cells were seeded 48 h before transfection onto opaque and transparent 96-well plate at a density of 10^4 cells per well and incubated at 37 °C in presence of 5% CO_2 atmosphere. Cells were grown to 80% confluence before being washed with 1x PBS and incubated with lipoplexes containing 3.6 μg of plasmid DNA in a volume of 45 μL in triplicate for 4 h at 37 °C in the presence of 5% CO_2 atmosphere. Complexes were then removed and the cells washed with 1× PBS before adding 100 μL of complete RPMI media. Cells were left to incubate for an additional 44 h. Following the incubation, transfection and cytotoxicity assays were carried out according to the below mentioned protocols.

β-Galactosidase assay and protein assay. Cells grown in an opaque 96-well plate were evaluated for β-galactosidase activity 48 h after transfection using a Beta-Glo® Assay System (Promega) according to the manufacturer's instructions. Luminescence was determined on a Perkin Elmer Precisely Wallac Envision 2104 Multilabel Plate reader (Perkin Elmer, Waltham, MA). β-Galactosidase activity was expressed as relative light units produced by the luminescence of luciferin, which was normalized for protein content. Total protein content was measured using Pierce® BCA Protein Assay (Pierce Biotechnology, Rockford, IL) according to the manufacturer's instructions. A calibration curve obtained from a bovine serum albumin standard solution was used to determine cellular protein content per well.

Cytotoxicity assay. The cytotoxicity associated with the lipoplex formulations at N/P ratios ranging from 0.5:1 to 10:1 was evaluated using the MTS (3-(4,5-dimethylthiazol-2-yl)-5-(3-carboxymethoxyphenyl)-2-(4-sulfophenyl)-2*H*-tetrazolium) assay. Forty-eight hours after the application of lipoplexes, CHO-K1 cells in the transparent 96-well plates were washed with 1× PBS, 50 μL of DMEM (phenol red-free media) and evaluated for cell viability using the CellTiter96® Aqueous One Solution Cell Proliferation Assay (Promega) according to the manufacturer's instructions. The absorbance of converted dye, which correlates with the number of viable cells, was measured at 492 nm using a Victor Envision high throughput plate reader. The percentage of viable cells was calculated as the absorbance ratio of treated to untreated cells.

3. Synthesis (Scheme 1)

3.1. Synthesis of (2-bromoethyl)(hexyl)(2-hydroxyethyl)phosphate (**4-6**)

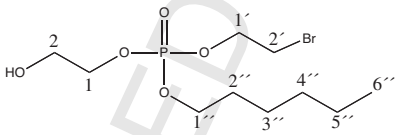

2-Chloro-1,3,2-dioxaphospholan (**3**) (1.25 equiv., 2.00 g, 15.8 mmol) was dissolved in dry CH_2Cl_2 (50 mL) and cooled on ice. Dry triethylamine (1.5 equiv., 1.94 g, 19.2 mmol) and 1-hexanol (1.31 g, 12.8 mmol) were introduced drop-wise and the mixture refluxed under N_2 for 16 h. After cooling to −20 °C Br_2 was added until the solution became permanent slight yellow. Dry triethylamine (2 mL) and ethyleneglycol (**1**) (5 mL) were added and the mixture refluxed for 12 h. Extraction of the mixture with water (3× 50 mL), drying with anhydrous Na_2SO_4, and vacuum concentration gave a residue, which, after flash-CC on silica with hexane/acetone 1:1 (v/v), gave **4-6** (1.38 g, 32%). TLC (toluene/acetone/MeOH, 6:1:1, v/v): R_f = 0.42. HRMS: $C_{10}H_{22}BrO_5P$ calcd. 333.0461 (M+H), found 333.0477. ^1H NMR, ^{13}C NMR and ^{31}P NMR in Supplemental Information.

3.2. Synthesis of (2-bromoethyl)(dodecyl)(2-hydroxyethyl)phosphate (**4-12**)

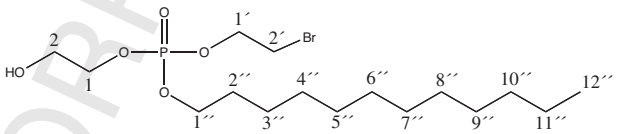

Phosphate triester **4-12** was obtained (250 mg, 5%) from 1-dodecanol (2.39 g 12.8 mmol) as described for **4-6**. TLC (toluene/acetone/MeOH 6:1:1, v/v): R_f = 0.38. HRMS: $C_{16}H_{34}BrO_5P$ calcd. 417.1400 (M+H), found 417.1420. ^1H NMR, ^{13}C NMR and ^{31}P NMR in Supplemental Information.

3.3. Synthesis of (2-bromoethyl)(tetradecyl)(2-hydroxyethyl)phosphate (**4-14**)

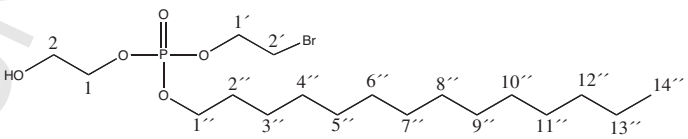

Phosphate triester **4-14** was obtained (1.22 g, 21%) from 1-tetradecanol (2.74 g, 12.8 mmol) as described for **4-6**. TLC (toluene/acetone/MeOH 6:1:1, v/v): R_f = 0.45. HRMS: $C_{18}H_{38}BrO_5P$ calcd. 445.1713 (M+H), found 445.1729. ^1H NMR, ^{13}C NMR and ^{31}P NMR in Supplemental Information.

Please cite this article in press as: Øpstad, C.L., et al., Novel cationic polyene glycol phospholipids as DNA transfer reagents—Lack of a structure–activity relationship due to uncontrolled self-assembling processes. Chem. Phys. Lipids (2014), http://dx.doi.org/10.1016/j.chemphyslip.2014.04.006

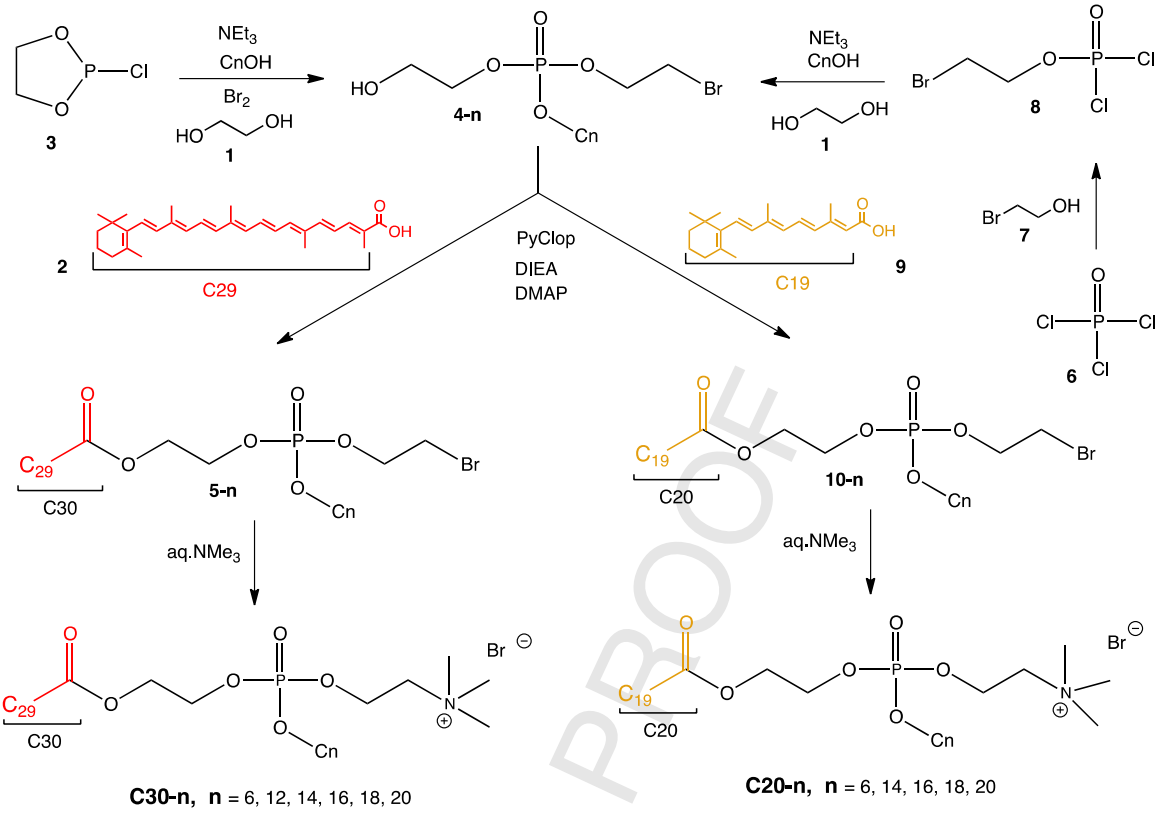

Scheme 1. Synthesis of cationic polyene glycol lipids C20-n and C30-n.

3.4. Synthesis of 2-bromoethyl dichlorophosphate (**8**)

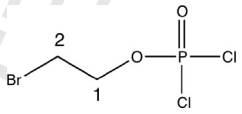

Fresh distilled 2-bromoethanol (**7**) (1.05 equiv., 6.08 g, 50 mmol) dissolved in dry CH_2Cl_2 (5 mL) was added drop-wise during 1 h to an ice-cooled solution of fresh distilled $POCl_3$ (**6**) (7.35 g, 48 mmol) dissolved in dry CH_2Cl_2 (10 mL). The reaction mixture was refluxed for 5 h. Vacuum-distillation (b.p. 66–69 °C, 0.4 mbar) gave **8** (10.4 g, 90%). HRMS: calcd. for $C_2H_4BrCl_2O_2P$ 241.8458 (M−1); found 241.8459. ^1H NMR, ^{13}C NMR and ^{31}P NMR in Supplemental Information.

3.5. Synthesis of (2-bromoethyl)(hexadecyl)(2-hydroxyethyl)phosphate (**4-16**)

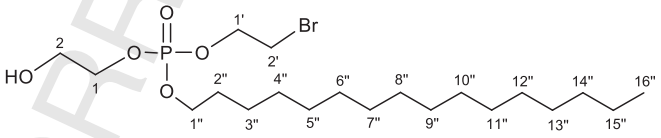

2-Bromoethyl dichlorophosphate (**8**) (1.49 equiv., 2.97 g; 0.0122 mol) was dissolved in anhydrous CH_2Cl_2 (20 mL) and cooled to 0 °C. Anhydrous triethylamine (1.98 equiv.; 1.642 g; 0.016 mol) was dissolved in anhydrous CH_2Cl_2 (10 mL) and drop wise added to the solution. 1-Hexadecanol (1 equiv., 2 g, 0.0082 mol) dissolved in anhydrous CH_2Cl_2 (20 mL) was drop wise added and the resulting mixture was refluxed for 5 h. Ethylene glycol (**1**) (2.19 equiv., 1.11 g; 0.0082 mol) was added and the mixture refluxed for 22 h, extracted with H_2O, dried over Na_2SO_4 and concentrated *in vacuo*. Purification by flash-CC on silica with hexane:acetone 1:1 (v/v) gave **4-16** (1.51 g, 39%). TLC (toluene/acetone/MeOH, 6:1:1, v/v): R_f = 0.47. HRMS: $C_{20}H_{42}BrO_5P$ calcd. 473.2024 (M+H), found 473.2024. ^1H NMR, ^{13}C NMR and ^{31}P NMR in Supplemental Information.

3.6. Synthesis of (2-bromoethyl)(octadecyl)(2-hydroxyethyl)phosphate (**4-18**)

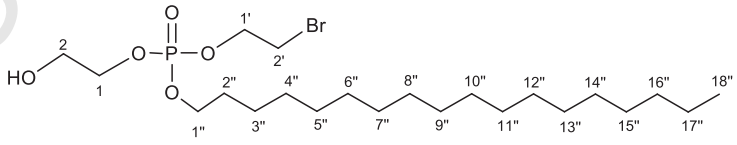

Please cite this article in press as: Øpstad, C.L., et al., Novel cationic polyene glycol phospholipids as DNA transfer reagents—Lack of a structure–activity relationship due to uncontrolled self-assembling processes. Chem. Phys. Lipids (2014), http://dx.doi.org/10.1016/j.chemphyslip.2014.04.006

Phosphate triester **4-18** was obtained (1.87 g, 34%) from 1-octadecanol (3.00 g, 11.0 mmol) as described for **4-16**. TLC (toluene/acetone/MeOH, 6:1:1, v/v): R_f = 0.44. HRMS: $C_{22}H_{46}BrO_5P$ calcd. 501.2333 (M+H), found 501.2334. ^{1}H NMR, ^{13}C NMR and ^{31}P NMR in Supplemental Information.

3.7. Synthesis of (2-bromoethyl)(icosyl)(2-hydroxyethyl)phosphate (**4-20**)

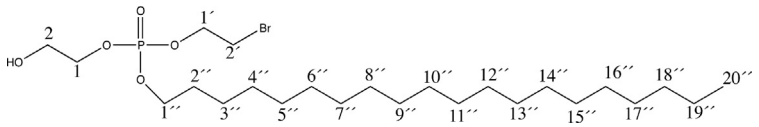

Phosphate triester **4-20** was obtained (44 g, 21%) from 1-icosanol (3.82 g, 12.819 mmol) as described for **4-6**. TLC (toluene/acetone/MeOH 6:1:1, v/v): R_f = 0.47. HRMS: $C_{24}H_{50}BrO_5P$ calcd. 528.2579, found 528.260. ^{1}H NMR, ^{13}C NMR and ^{31}P NMR in Supplemental Information.

3.8. Synthesis of 2-((2-bromoethoxy)(hexyloxy)phosphoryl)ethoxy-retinoate (**10-6**)

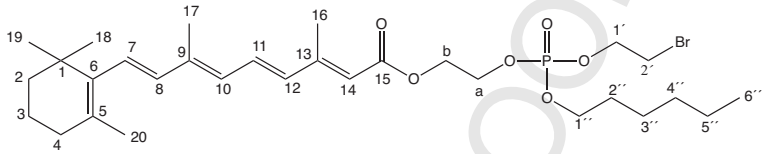

Retinoic acid (**9**) (200 mg, 0.666 mmol), **4-6** (266 mg, 0.799 mol), chlorotripyrrolidinophosphonium hexafluorophosphate (PyCloP, 1.25 equiv., 349 mg, 0.868 mmol), *N*-ethyl diisopropylamine (DIEA, 0.65 equiv., 58 mg, 0.451 mmol), and DMAP (1.25 equiv., 106 mg, 0.868 mmol) were dissolved in dry CH_2Cl_2 (50 mL) and the mixture was refluxed under N_2 for 24 h. Extraction of the mixture with water (2× 50 mL), aqueous HBr (0.1 M, 2× 50 mL), and water (2× 50 mL), drying over anhydrous Na_2SO_4 and concentration gave a residue, which, after flash-CC on silica with a toluene-acetone gradient, gave **10-6** (377 mg, 92%). TLC (toluene/acetone/MeOH 6/1/1, v/v): R_f = 0.68. UV/vis (CH_2Cl_2): λ_{max} = 370 nm. HRMS: $C_{30}H_{48}BrO_6P$ calcd. 615.2445 (M+H), found 615.2467. ^{1}H NMR, ^{13}C NMR and ^{31}P NMR in Supplemental Information.

3.9. Synthesis of 2-((choline)(hexyloxy)phosphoryloxy)ethoxy-retinoate (**C20-6**)

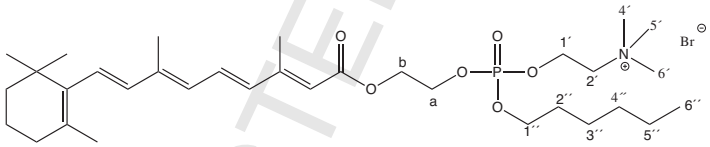

10-6 (358 mg, 0.582 mmol), was dissolved in $CHCl_3$/*i*PrOH/DMF (3/5/5, v/v, 50 mL), NMe_3 (45% in water, 10 mL) was added and the mixture stirred at room temperature under N_2 for 4 days. Purification by flash-CC gave **C20-6** (288 mg, 74%). TLC ($CHCl_3$/MeOH/H_2O 40:50:10, v/v): R_f = 0.28. UV/vis (CH_2Cl_2): λ_{max} = 368 nm. HRMS: $C_{33}H_{57}NO_6P$ calcd. 594.3924 (M^+), found 594.3926. ^{1}H NMR, ^{13}C NMR and ^{31}P NMR in Supplemental Information.

3.10. Synthesis of 2-((2-bromoethoxy)(tetradecyloxy)phosphoryloxy)ethoxy-retionoate (**10-14**)

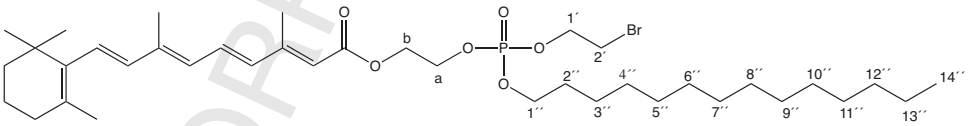

Retinoic acid (**9**) (200 mg, 0.666 mmol) and **4-14** (356 mg, 0.799 mmol) were reacted as described for **10-6** giving **10-14** (423 mg, 87%). TLC (toluene/acetone/MeOH 6:1:1, v/v): R_f = 0.80. UV/vis (CH_2Cl_2): λ_{max} = 369 nm. HRMS: $C_{38}H_{64}BrO_6P$ calcd. 727.3697 (M+H), found 727.3730. ^{1}H NMR, ^{13}C NMR and ^{31}P NMR in Supplemental Information.

3.11. Synthesis of 2-((choline)(tetradecyloxy)phosphoryloxy)ethoxy-retinoate (**C20-14**)

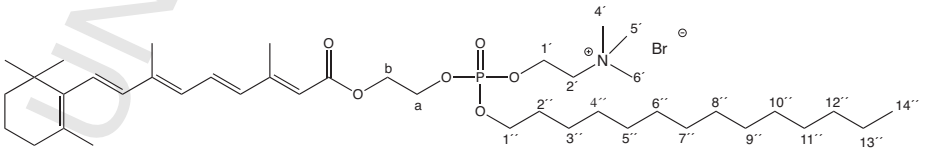

10-14 (432 mg, 0.594 mmol) was reacted as described for **C20-6**. Purification by flash-CC gave **C20-14** (256 mg, 55%). TLC ($CHCl_3$/MeOH/H_2O 40:50:10, v/v): R_f = 0.38. UV/vis (CH_2Cl_2): λ_{max} = 371 nm. HRMS: $C_{41}H_{73}NO_6P$ calcd. 706.5176 (M^+), found 706.5187. ^{1}H NMR, ^{13}C NMR and ^{31}P NMR in Supplemental Information.

Please cite this article in press as: Øpstad, C.L., et al., Novel cationic polyene glycol phospholipids as DNA transfer reagents—Lack of a structure–activity relationship due to uncontrolled self-assembling processes. Chem. Phys. Lipids (2014), http://dx.doi.org/10.1016/j.chemphyslip.2014.04.006

3.12. Synthesis of 2-((2-bromoethoxy)(hexadecyloxy)phosphoryloxy)ethoxy-retionoate (**10-16**)

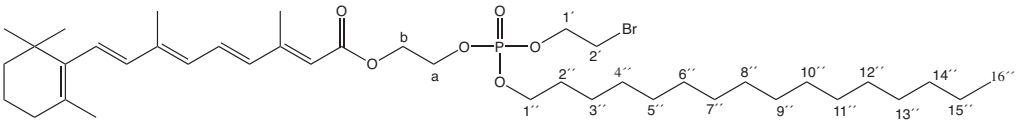

Retinoic acid (**9**) (515 mg, 1.7 mmol) and **4-16** (1.24 equiv., 1 g, 2.10 mmol) were reacted as described for **10-6** giving **10-16** (990 mg, 69%). TLC (toluene/acetone/MeOH 6/1/1, v/v): R_f = 0.61. UV/vis (CH_2Cl_2): λ_{max} = 355 nm. HRMS: $C_{40}H_{68}BrO_6P$ calcd. 754.3920 (M+H), found 754.3921. ^{1}H NMR, ^{13}C NMR and ^{31}P NMR in Supplemental Information.

3.13. Synthesis of 2-((choline)(hexadecyloxy)phosphoryloxy)ethoxy-retinoate (**C20-16**)

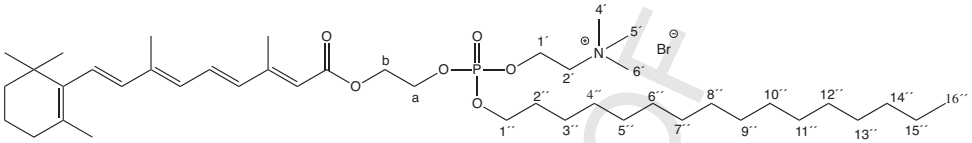

10-16 (400 mg, 0.52 mmol) was reacted as described for **C20-6**. Purification by flash-CC gave **C20-16** (450 mg, 99%). TLC ($CHCl_3$/MeOH/H_2O 70:30:3, v/v): R_f = 0.81. UV/vis (CH_2Cl_2): λ_{max} = 356 nm. HRMS: $C_{43}H_{77}NO_6P$ calcd. 734.5476 (M^+), found 734.5473. ^{1}H NMR, ^{13}C NMR and ^{31}P NMR in Supplemental Information.

3.14. Synthesis of 2-((2-bromoethoxy)(octadecyloxy)phosphoryloxy)ethoxy-retionoate (**10-18**)

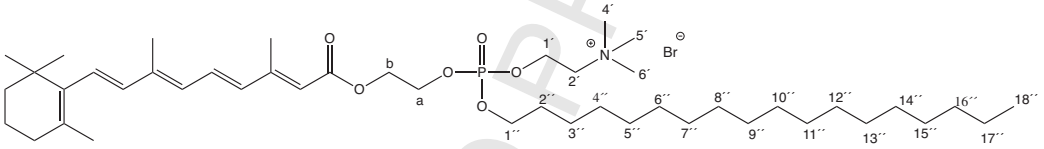

Retinoic acid (**9**) (500 mg, 1.6 mmol) and **4-18** (1.24 equiv., 1 g, 2.10 mmol) were reacted as described for **10-6** giving **10-18** (949 mg, 75%). TLC (toluene/acetone//MeOH 6/1/1, v/v): R_f = 0.65. UV/vis (CH_2Cl_2): λ_{max} = 355 nm. HRMS: $C_{42}H_{72}BrO_6P$ calcd. 782.4245 (M^+), found 782.4245. ^{1}H NMR, ^{13}C NMR and ^{31}P NMR in Supplemental Information.

3.15. Synthesis of 2-((choline)(octadecyloxy)phosphoryloxy)ethoxy-retinoate (**C20-18**)

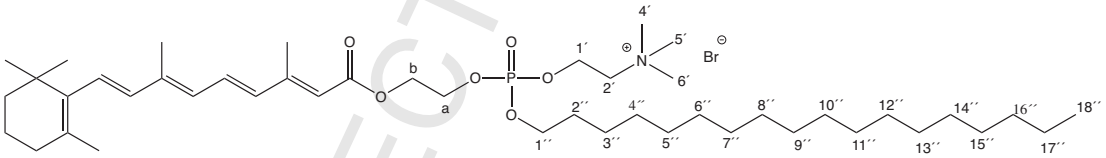

10-18 (350 mg, 0.44 mmol) was reacted as described for **C20-6**. Purification by flash-CC gave **C20-18** (300 mg, 81%). TLC ($CHCl_3$/MeOH/H_2O 70:30:3, v/v): R_f = 0.84. UV/vis (CH_2Cl_2): λ_{max} = 355 nm. HRMS: $C_{45}H_{81}NO_6P$ calcd. 762.5781 (M^+), found 762.5779. ^{1}H NMR, ^{13}C NMR and ^{31}P NMR in Supplemental Information.

3.16. Synthesis of 2-((2-bromoethoxy)(icosyloxy)phosphoryloxy)ethoxy-retinoate (**10-20**)

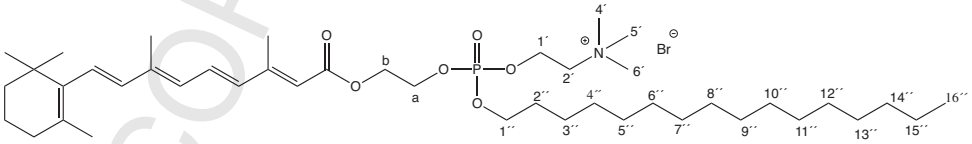

Retinoic acid (**9**) (200 mg, 0.666 mmol) and **4-20** (423 mg, 0.799 mmol) were reacted as described for **10-6** giving **10-20** (478 mg, 88%). TLC: (toluene/acetone/MeOH 6:1:1, v/v): R_f = 0.85. UV/vis (CH_2Cl_2): λ_{max} = 370 nm. HRMS: $C_{44}H_{76}BrO_6P$ calcd.811.4636 (M+H), found 811.4668. ^{1}H NMR, ^{13}C NMR and ^{31}P NMR in Supplemental Information.

3.17. Synthesis of 2-((choline)(icosyloxy)phosphoryloxy)ethoxy-retinoate (**C20-20**)

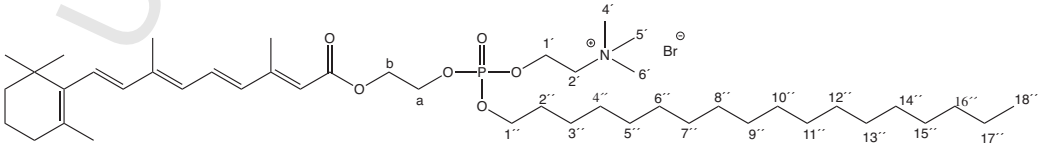

Please cite this article in press as: Øpstad, C.L., et al., Novel cationic polyene glycol phospholipids as DNA transfer reagents—Lack of a structure–activity relationship due to uncontrolled self-assembling processes. Chem. Phys. Lipids (2014), http://dx.doi.org/10.1016/j.chemphyslip.2014.04.006

10-20 (460 mg, 0.566 mmol), was reacted as described for **C20-6**. Purification by flash-CC gave **C20-20** (362 mg, 74%). TLC ($CHCl_3$/MeOH/H_2O 40:50:10, v/v): R_f = 0.42 UV/vis (CH_2Cl_2): λ_{max} = 369 nm. HRMS: $C_{47}H_{85}NO_6P$ calcd.790.6115 (M^+), found 790.6125. ^1H NMR, ^{13}C NMR and ^{31}P NMR in Supplemental Information.

3.18. Synthesis of β-apo-8′-carotenoic acid (**2**)

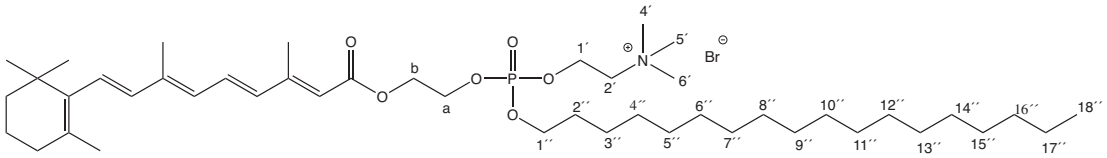

Hydrolysis of β-apo-8′-carotenoate gave **2** in 90% yield. ^1H NMR: in accordance with Ref. Larsen et al. (1998).

3.19. Synthesis of 2-((2-bromoethoxy)(hexyloxy)phosphoryloxy)ethoxy-β-apo-8′-carotenoate (**5-6**)

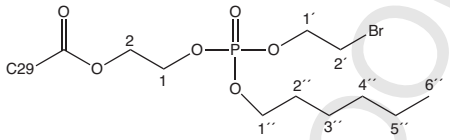

β-Apo-8′-carotenoic acid (**2**) (300 mg, 0.694 mmol), **4-6** (1.2 equiv., 257 mg, 0.773 mmol), chlorotripyrrolidinophosphonium hexafluorophosphate (PyCloP, 1.25 equiv., 349 mg, 0.868 mmol), *N*-ethyl diisopropylamine (DIEA, 0.65 equiv., 58 mg, 0.451 mmol), and DMAP (1.25 equiv., 106 mg, 0.868 mmol) were dissolved in dry CH_2Cl_2 (50 mL) and the mixture was refluxed under N_2 for 24 h. Extraction of the mixture with water (2× 50 mL), aqueous HBr (0.1 M, 2× 50 mL), and water (2× 50 mL), drying over anhydrous Na_2SO_4 and concentration gave a residue, which, after flash-CC on silica with a toluene–acetone gradient, gave **5-6** (322.3 mg, 62%). TLC (toluene/acetone/MeOH 6:1:1, v/v): R_f = 0.68. UV/vis (CH_2Cl_2): λ_{max} = 453 nm. MS: 746.85 + 748.85 (1:1, M^+); HRMS: $C_{40}H_{60}BrO_6P$ calcd. 748.32993 (M^+), found 748.33023. ^1H NMR, ^{13}C NMR and ^{31}P NMR in Supplemental Information.

3.20. Synthesis of 2-((choline)(hexyloxy)phosphoryloxy)ethoxy-β-apo-8′-carotenoate (**C30-6**)

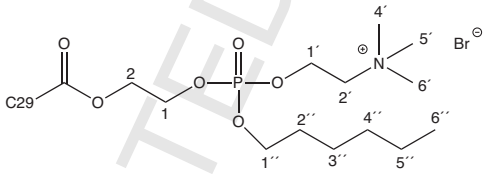

Carotenoate **5-6** (322 mg, 0.43 mmol) was dissolved in $CHCl_3$/iPrOH/DMF (3/5/5, v/v, 50 mL), NMe_3 (45% in water, 10 mL) was added and the mixture stirred at room temperature under N_2 for 4 days. Flash-CC on neutral Al_2O_3 gave **C30-6** (264 mg, 77%). TLC ($CHCl_3$/MeOH/H_2O 70:30:3, v/v): R_f = 0.08. UV/vis (CH_2Cl_2): λ_{max} = 458 nm. HRMS: $C_{43}H_{69}NO_6P$ calcd. 726.4803 (M^+), found 726.4869. ^1H NMR, ^{13}C NMR and ^{31}P NMR in Supplemental Information.

3.21. Synthesis of 2-((2-bromoethoxy)(dodecyloxy)phosphoryloxy)ethoxy-β-apo-8′-carotenoate (**5-12**)

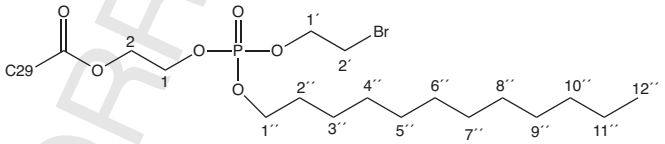

β-Apo-8′-carotenoic acid (**2**) (200 mg, 0.459 mmol) and **4-12** (1.2 equiv., 230 mg, 0.550 mmol) were reacted as described for **5-6** giving **5-12** (200.7 mg, 53%). TLC (hexane/acetone 8:2, v/v): R_f = 0.30. UV/vis (CH_2Cl_2): λ_{max} = 457 nm. MS (EI): 830.1 + 832.2 (1:1, M^+). HRMS: $C_{46}H_{72}BrO_6P$ calcd. 830.42500 (M^+), found 830.42748. ^1H NMR, ^{13}C NMR and ^{31}P NMR in Supplemental Information.

3.22. Synthesis of 2-((choline)(dodecyloxy)phosphoryloxy)ethoxy-β-apo-8′-carotenoate (**C30-12**)

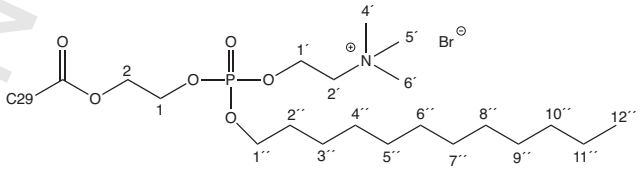

5-12 (200.7 mg, 0.241 mmol) was reacted as described for **C30-6**. Purification by flash-CC gave **C30-12** (130 mg, 61%). TLC ($CHCl_3$/MeOH/H_2O 70/30/3, v/v): R_f = 0.47. UV/vis (CH_2Cl_2): λ_{max} = 458 nm. HRMS: $C_{49}H_{81}NO_6P$ calcd. (M^+) 810.5802 (M^+), found 810.5793. ^1H NMR, ^{13}C NMR and ^{31}P NMR in Supplemental Information.

Please cite this article in press as: Øpstad, C.L., et al., Novel cationic polyene glycol phospholipids as DNA transfer reagents—Lack of a structure–activity relationship due to uncontrolled self-assembling processes. Chem. Phys. Lipids (2014), http://dx.doi.org/10.1016/j.chemphyslip.2014.04.006

3.23. Synthesis of 2-((2-bromoethoxy)(tetradecyloxy)phosphoryloxy)ethoxy-β-apo-8′-carotenoate (**5-14**)

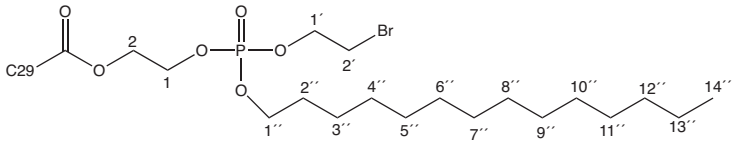

β-Apo-8′carotenoic acid (**2**) (300 mg, 0.694 mmol) and **4-14** (1.2 equiv., 344 mg, 0.773 mmol) were reacted as described for **5-6** to **5-14** (425 mg, 71%). TLC (hexane/acetone 8:2), v/v: R_f = 0.27. UV/vis (CH_2Cl_2): λ_{max} = 457 nm. ^{1}H NMR, ^{13}C NMR and ^{31}P NMR in Supplemental Information.

3.24. Synthesis of 2-((choline)(tetradecyloxy)phosphoryloxy)ethoxy-β-apo-8′-carotenoate (**C30-14**)

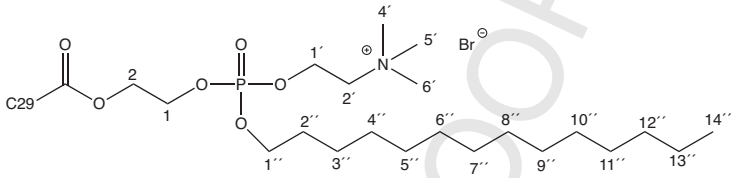

5-14 (400 mg, 0.465 mmol) was reacted as described for **C30-6**. Purification by flash-CC gave **C30-14** (242 mg, 57%).TLC ($CHCl_3$/MeOH/H_2O 70:30:3, v/v): R_f = 0.68. UV/vis (CH_2Cl_2): λ_{max} = 461 nm. HRMS: $C_{51}H_{85}NO_6P$ calcd. 838.6115 (M^+), found 838.6121. ^{1}H NMR, ^{13}C NMR and ^{31}P NMR in Supplemental Information.

3.25. Synthesis of 2-((2-bromoethoxy)(hexadecyloxy)phosphoryloxy)ethoxy-β-apo-8′-carotenoate (**5-16**)

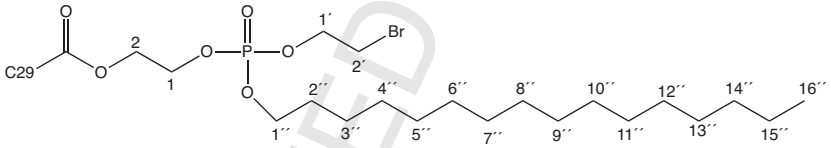

β-Apo-8′-carotenoic acid (**2**) (450 mg, 1.04 mmol) and **4-16** (2.39 equiv., 1.174 mg, 2.48 mmol) were reacted as described for **5-6** giving **5-16** (631 mg, 68%). TLC (toluene/acetone/MeOH 6:1:1, v/v): R_f = 0.80. UV/vis (CH_2Cl_2): λ_{max} = 455 nm. HRMS: $C_{50}H_{80}BrO_6P$ calcd. 886.4869 (M+H), found 886.4869. ^{1}H NMR, ^{13}C NMR and ^{31}P NMR in Supplemental Information.

3.26. Synthesis of 2-((choline)(hexadecyloxy)phosphoryloxy)ethoxy-β-apo-8′-carotenoate (**C30-16**)

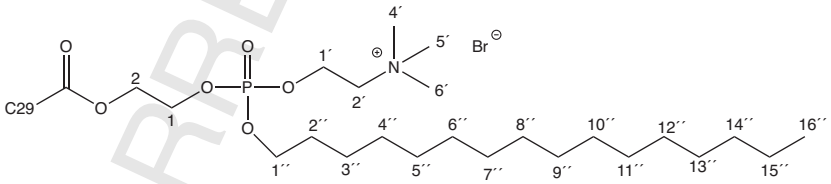

5-16 (200 mg, 0.225 mmol) was reacted as described for **C30-6**. Purification by flash-CC gave **C30-16** (155 mg, 72%). TLC ($CHCl_3$/MeOH/H_2O 70:30:3, v/v): R_f = 0.62. UV/vis (CH_2Cl_2): λ_{max} = 456 nm. HRMS: $C_{53}H_{89}NO_6P$ calcd. 866.6422 (M^+), found 866.6423. ^{1}H NMR, ^{13}C NMR and ^{31}P NMR in Supplemental Information.

3.27. Synthesis of 2-((2-bromoethoxy)(octadecyloxy)phosphoryloxy)ethoxy-β-apo-8′-carotenoate (**5-18**)

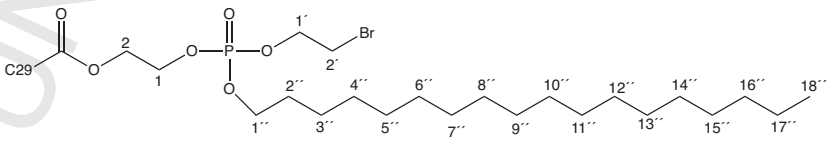

β-Apo-8′carotenoic acid (**2**) (670 mg, 1.54 mmol), **4-18** (2.39 equiv., 1856 mg, 3.70 mmol) were reacted as described for **5-6** giving **5-18** (858 mg, 61%). TLC (toluene/acetone/MeOH 6:1:1, v/v): R_f = 0.75. UV/vis (CH_2Cl_2): λ_{max} = 454 nm. HRMS: $C_{52}H_{84}BrO_6P$ calcd. 914.5196 (M^+), found 914.5189. ^{1}H NMR, ^{13}C NMR and ^{31}P NMR in Supplemental Information.

Please cite this article in press as: Øpstad, C.L., et al., Novel cationic polyene glycol phospholipids as DNA transfer reagents—Lack of a structure–activity relationship due to uncontrolled self-assembling processes. Chem. Phys. Lipids (2014), http://dx.doi.org/10.1016/j.chemphyslip.2014.04.006

3.28. Synthesis of 2-((choline)(octadecyloxy)phosphoryloxy)ethoxy-β-apo-8′-carotenoate (**C30-18**)

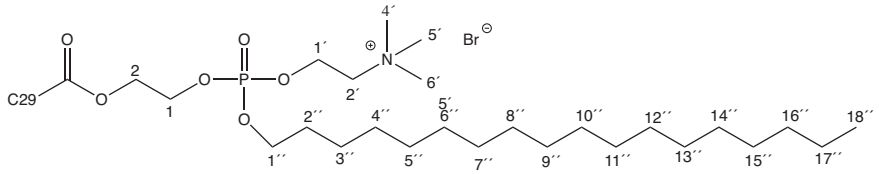

5-18 (240 mg, 0.261 mmol) was reacted as described for **C30-6**. Purification by flash-CC gave **C30-18** (200 mg, 78%). TLC ($CHCl_3$/MeOH/H_2O 70:30:3, v/v): R_f = 0.82. UV/vis (CH_2Cl_2): λ_{max} = 455 nm. HRMS: $C_{55}H_{93}NO_6P$ calcd. 894.6729 (M^+), found 894.6728. ^1H NMR, ^{13}C NMR and ^{31}P NMR in Supplemental Information.

3.29. Synthesis of 2-((2-bromoethoxy)(icosyloxy)phosphoryloxy)ethoxy-β-apo-8′-carotenoate (**5-20**)

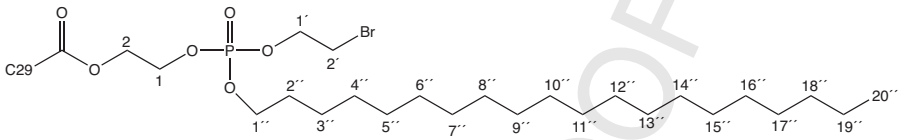

β-Apo-8′-carotenoic acid (**2**) (397 mg, 0.919 mmol) and **4-20** (340 mg, 0.584 mmol) were reacted as described for **5-6** giving **5-20** (333 mg, 62%). TLC (hexane/acetone 8:2, v/v): R_f = 0.28. UV/vis (CH_2Cl_2): λ_{max} = 458 nm. HRMS: $C_{54}H_{88}BrO_6P$ calcd. 945.5568, found 945.5547 (M+H). ^1H NMR, ^{13}C NMR and ^{31}P NMR in Supplemental Information.

3.30. Synthesis of 2-((choline)(icosyloxy)phosphoryloxy)ethoxy-β-apo-8′-carotenoate (**C30-20**)

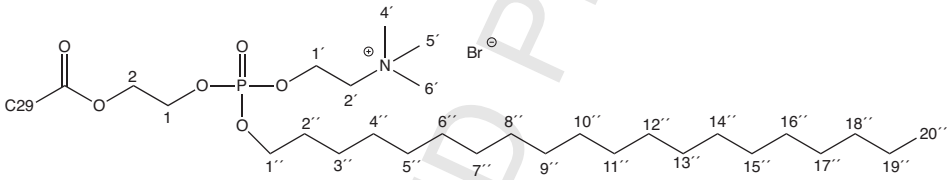

5-20 (300 mg, 0.317 mmol) was reacted as described for **C30-6**. Purification by flash-CC gave **C30-20** (303 mg, 95%). TLC ($CHCl_3$/MeOH/H_2O 70:30:3, v/v): R_f = 0.78. UV/vis (CH_2Cl_2): λ_{max} = 459 nm. HRMS: $C_{57}H_{97}NO_6P$ calcd. 922.7054, found 922.7048 (M^+). ^1H NMR, ^{13}C NMR and ^{31}P NMR in Supplemental Information.

4. Results and discussion

4.1. Synthesis

Cationic lipids are often identified with phospholipids and phospholipids are habitually recognized as glycerophospholipids) (Foss et al., 2003, 2005a). Yet, the glycerol scaffold complicates structure–activity studies by possible formation of mono- and di-glycerol isomers and enantiomers, and by inter- and intra-molecular acyl migration (Chang et al., 1997; Mangroo and Gerber, 1988). We, therefore, replaced the glycerol (propanetriol n = 3) backbone with glycol (**1**) (ethanediol n = 2; glycolphospholipids occur in minor amounts in natural lipids) (Bergelson, 1970). We further exchanged one of the flexible saturated acyl chains characteristically located in lipid gene carriers (Koynova and Tenchov, 2009) with β-apo-8′-carotenoic acid ($C_{30:9}$) (**2**) (C30-acid, food color E160f) and retinoic acid ($C_{20:5}$) (**9**) (Scheme 1). Keeping the glycol unit, the polyene chains and the charged head group constant, the length of the phosphate ester alkyl chain was varied (C_6, C_{12}, C_{14}, C_{16}, C_{18}, C_{20}); we acquired two C20-n and C30-n series (Fig. 1 and Scheme 1). Cationic phospholipids bearing different chains or chains with conjugated unsaturation are rarely examined (Adami et al., 2011; Koynova et al., 2009; Zhi et al., 2010). The dependence of transfection efficiency on phosphate ester alkyl chains has earlier been accentuated (Rosenzweig et al., 2000).

Reacting chlorodioxaphospholane (**3**) with glycol (**1**) and subsequent addition of the appropriate alcohol C_n-OH and Br_2 gave intermediate phosphate **4-n** (Byun and Bittman, 1996), which with C30-acid **2** and the coupling reagents chlorotripyrrolidinophosphonium hexafluorophosphate (PyCloP) (Coste et al., 1994), diisopropylethylamine (DIEA) and 4-dimethylaminopyridine (DMAP) formed bromophosphotriester **5-n**. Aminolysis of **5-n** gave **C30-6**, **C30-12**, **C30-14** and **C30-20** (Scheme 1). Phosphorous diesters were retrieved as byproducts and bromine reacted promiscuously with phosphorous and the exo- and endocyclic methylene groups next to the P—O-bonds in phospholane **3** (Predvoditilev et al., 2001). Otherwise, trichlorophosphate (**6**) was reacted with bromoethanol (**7**) to bromophosphate **8**, which with glycol (**1**) and alcohol C_n-OH gave again intermediate **4-n**. By these sequences **C30-16** and **C30-18** were obtained. Similarly, phosphate **4-n** reacted with retinoic acid **9** to the C20-n compounds.

4.2. Molecular structure

The combination of rigidity and flexibility in the new lipids is exemplary demonstrated for **C30-14** (Fig. 3). Diverse conformational arrangements of acyl chains have been previously noticed in a zwitterionic phospholipid with a hexatriene chain (Ryhänen, 2006, p. 55). Since molecules with flexible chains are prone to variation in length, molecular volume figures as a more appropriate expression to account for chain extension (Fig. 4).

Please cite this article in press as: Øpstad, C.L., et al., Novel cationic polyene glycol phospholipids as DNA transfer reagents—Lack of a structure–activity relationship due to uncontrolled self-assembling processes. Chem. Phys. Lipids (2014), http://dx.doi.org/10.1016/j.chemphyslip.2014.04.006

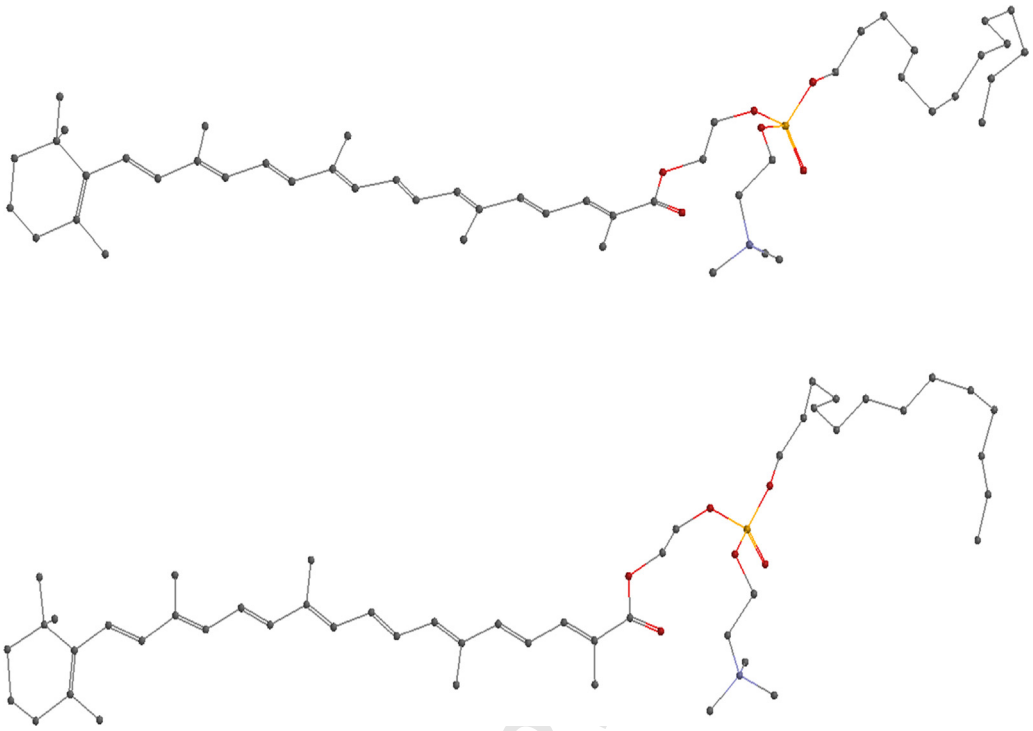

Fig. 3. Hypothetical structures of rigid polyene chains and flexible saturated alkyl chains in **C30-14**.

4.3. Surface properties

The surface tension γ of the synthesized amphiphilic phospholipid surfactants was determined with a tensiometer (Pt-plate). Calculation of the tensiometric data assessed the critical aggregation concentration c_M, the area per molecule at the filled monolayer a_m and other associated data such as γ_{c_M}, surface concentration Γ, free energy of aggregation ΔG^0_{ag} and adsorption ΔG^0_{ad}, surfactant performance indicator AMER (Skrylev et al., 2000), equilibrium constants for aggregation and adsorption k_{ag} and k_{ad} (Tables 1 and SI 1) (Foss et al., 2005b,c). The surface area a_m was established assuming no dissociation of the molecules in water (one species) or complete dissociation (two species). The values for a_m, supposing complete dissociation, were too high and in variance with molecular calculations indicating that the cationic molecules aggregate with tightly attached counter ions. The importance of tensiometric data for controlling gene transfer has been previously demonstrated by investigating Langmuir–Blodgett films (Antipina et al., 2009).

C20-16 is most surface active, decreasing the surface tension γ of water to 35 mN/m, whereas **C20-20** and **C30-14** are not effective surfactants with $\gamma = 62$ and 63 mN/m, respectively (Table 1 and Fig. 5). **C20-16** aggregates in water at low concentration ($c_M = 10.6\ \mu M$), **C20-20** is much more soluble with an aggregation concentration of 75 μM. The observation in prior studies that c_M of most surfactants decreases linearly with the number of carbon atoms in a chain is not reproduced with the C20-n and C30-n compounds (Shinoda, 1963; Yoshimura et al., 2012). The surface area a_m is rather similar, except for **C20-14** and **C30-14** with unexpected large a_m values (Fig. 6).

The hydrophilic chains in the C30-n series can adopt a “closed V” or a “stretched V”-shaped-conformation upon rotation about the oxygen—carbon bond of the phosphate ester acyl side chain (Fig. 7). The reasons why **C20-14** and **C30-14** orient differently are not evident. Analogous large surface areas have been detected with polyene bolaamphiphiles (Breukers et al., 2009). The comparison of the calculated molecular volumes, which are independent of chain orientation, revealed that ECP is equal to

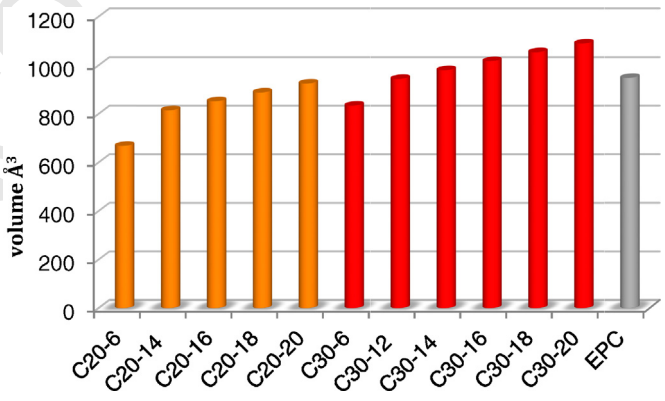

Fig. 4. Molecular volume (Å^3) of Cn-n compounds and EPC. **C30-12** and EPC have comparable molecular volumes (spartan08, semi empirical PM3).

Table 1
Q10 Surface property data of C20-n and C30-n.

	c_M (μM)	γ_c (mN/m)	Γ (μmol/m^2)	a_m (Å^2)
C20-6	31.7	46	2.05	81
C20-14	50	57	1.2	139
C20-16	10.6	35	2.32	72
C20-18	13	48	2.63	63
C20-20	75	63	2.6	63
C30-2	23.3	49	2.6	64
C30-6	19	53	2.97	56
C30-12	46.6	53	1.93	86
C30-14	41.7	62	0.87	191
C30-16	46	49	2.95	56
C30-18	16	42	2.61	64
C30-20	18.9	47	2.1	79

[a]Ref. Øpstad et al. (2013).

4.4. Aggregation

Aggregation of the C20-n and C30-n phospholipids started at irregular concentrations c_M (Table 1) and the morphology of the formed aggregates was hardly foreseeable, e.g. resulting for **C30-2** in rods, spheroids and cones (Øpstad et al., 2013). It is assumed that the other C20-n and C30-n lipids similarly self-assemble in water to polymorphic particles. Independent of their morphology, aggregates are characterized by their absorption spectrum reflecting the molecular arrangement in the aggregation unit (Foss et al., 2005a), e.g. the aqueous aggregate dispersion of **C30-14** absorbed at lower wavelengths than a molecular solution in organic solvents, suggesting an exitonic card-pack association of the molecules characterized as H-aggregates (**C30-14** in EtOH λ_{max} = 444 nm, **C30-14** in H_2O (H-aggregate) λ_{max} = 400 nm (Fig. 8) (Horn and Rieger, 2001; Wang et al., 2012). Aggregation depends on subtle conditions and amphiphilic molecules can also adopt head-to tail arrangements leading to higher absorbing *J*-aggregates. Such details in molecule arrangements are not easily distinguished in saturated lipids or in lipids with non conjugated double bonds (Sliwka et al., 2010).

Adding water to concentrated solvent solutions of the C30-n lipids allowed detecting the aggregation concentration c_{ag}; correspondingly, adding organic solvents to aqueous C30-n dispersions assessed the concentration of aggregate disruption. The monomer–aggregate equilibrium for **C30-14** was, for instance, found at 31% EtOH and 69% H_2O (Fig. 8).

4.5. Liposomes

Thin films of pure cationic lipids or mixtures of cationic lipids with co-lipids, DOPE or cholesterol, were hydrated initiating the formation of liposomes. Cholesterol and zwitterionic DOPE (thought to have a role in the protection of nucleic acids and promotion of transfection, Fig. 2) (Dabkowska et al., 2012; Hirsch-Lerner et al., 2005; Pozzi et al., 2012) were paired with the C20-n and C30-n compounds at a constant

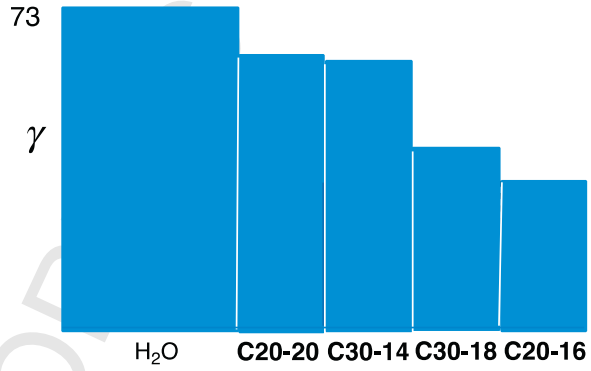

Fig. 5. Maximum and minimum reduction of water surface tension (γ = 73 mN/m) with surface active C20-n and C30-n compounds.

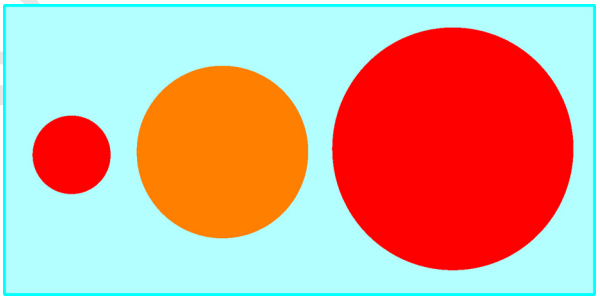

Fig. 6. Molecule area a_m at the water surface of **C30-16** (left, representing roughly the average of most C20-n and C30-n molecules), of **C20-14** (center) and **C30-14** (right).

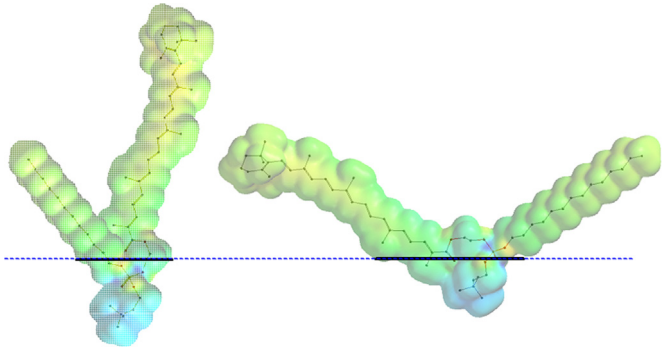

Fig. 7. Hypothetically oriented **C30-12** (closed V) and **C30-14** (stretched V) at the water surface, the black line — indicates the diameter of the surface area a_m at the water surface ▬ ▬ ▬ ▬ (semi-empirical, AM1 in Spartan 08, Wavefunction, Irvine, California, USA).

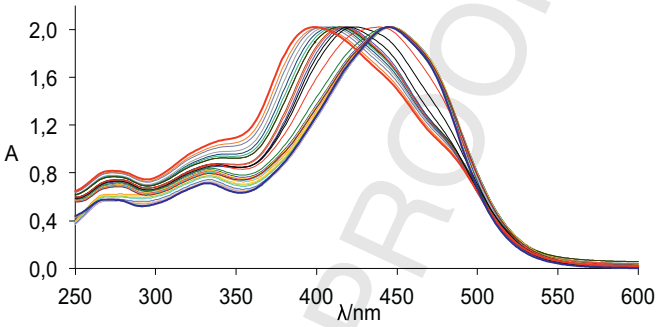

Fig. 8. Monomolecular solution of **C30-14** in EtOH ___ . Adding H_2O initiate formation of H-aggregates ___ . Aggregate dispersion of **C30-14** in H_2O ___ . Adding EtOH disrupts the aggregates forming a monomolecular solution ___ . The aggregation concentration (% H_2O in EtOH) c_{ag} = 69 (in MeCN c_{ag} = 74). (For interpretation of the references to color in this figure legend, the reader is referred to the web version of the article.)

molar ratio of 3:2 (lipid/co-lipid). The hydrodynamic radius and polydispersity index (PdI) of the liposomes was ascertained by dynamic light scattering (DLS). **C30-16** appeared as the smallest liposome (d_H = 70 nm) and liposome **C20-18** as the largest (d_H = 1640 nm, Table 2). Within the cholesterol series **C20-18**/Chol formed the smallest and **C30-20**/Chol the largest liposomes (d_H = 170 nm and d_H = 1400 nm, respectively). The high variance in the polydispersity index of the pure liposomes (PdI = 0.2–1) was reduced in the liposomes with DOPE to a PdI range of 0.3–0.6. The EPC-containing liposomes had low polydispersity and small sizes, as reported elsewhere (Øpstad et al., 2013), suggesting that the variability in liposome size and polydispersity among C30-n and C30-n liposomes was inherent to their self-association properties. Thus, the polyene cationic lipids, regardless of formulation, yielded a range of liposome with no obvious structure–property relationship. Our results contrast with the outcome of identical sized liposomes independent of chemical structure (Ivanova et al., 2013)

Having completed a thorough analysis of physical and chemical characteristics of the novel lipids as well as an analysis of liposome formation, the data comparing structure and property can be viewed graphically. The dataset manifests no structure–property relationship of the new lipids (Fig. 9).

4.6. Lipoplexes

Negatively charged DNA was subsequently added to cationic liposomes; lipoplexes were obtained, mediated by electrostatic interactions and hydrophobic effects. Lipoplex formulations are described in terms of defined amine:phosphate (N/P) or molar charge ratios (+/−). In this study, N/P ratios of 0.5:1, 1.5:1, 3.0:1, 5.0:1 and, in some cases, 10:1 were evaluated. Dynamic light scattering was employed to characterize lipoplexes. Measurements indicated a wide range of hydrodynamic diameters, d_H (Table SI 2). C20-n lipoplexes were smaller on average when the saturated chain was shorter (i.e. **C20-14**), but as this chain increased in length, formulations with cholesterol produced reduced lipoplexes, i.e. **C20-18**/Chol and **C20-20**/Chol. C30-n lipoplexes were usually smaller without co-lipid and largest with cholesterol. The

Table 2
Hydrodynamic diameter d_H (nm) of liposomes and polydispersity index (PdI) measured by DLS. **C30-6** was omitted for instability reasons.

Cationic lipid	Liposome		Liposome/DOPE		Liposome/Chol	
	d_H (nm)	PdI	d_H (nm)	PdI	d_H (nm)	PdI
EPC	120	0.6	490	0.6	300	0.4
C20-14	180	0.4	1015	0.6	550	0.7
C20-16	480	0.8	350	0.3	365	0.8
C20-18	1645	0.8	510	0.5	170	0.4
C20-20	815	0.5	670	0.6	260	0.4
C30-12	270	1	275	0.5	640	0.4
C30-14	375	0.5	382	0.6	397	0.8
C30-16	75	0.5	293	0.4	265	0.4
C30-18	230	0.8	300	0.4	260	0.4
C30-20	205	0.2	880	0.6	1400	0.8

Please cite this article in press as: Øpstad, C.L., et al., Novel cationic polyene glycol phospholipids as DNA transfer reagents—Lack of a structure–activity relationship due to uncontrolled self-assembling processes. Chem. Phys. Lipids (2014), http://dx.doi.org/10.1016/j.chemphyslip.2014.04.006

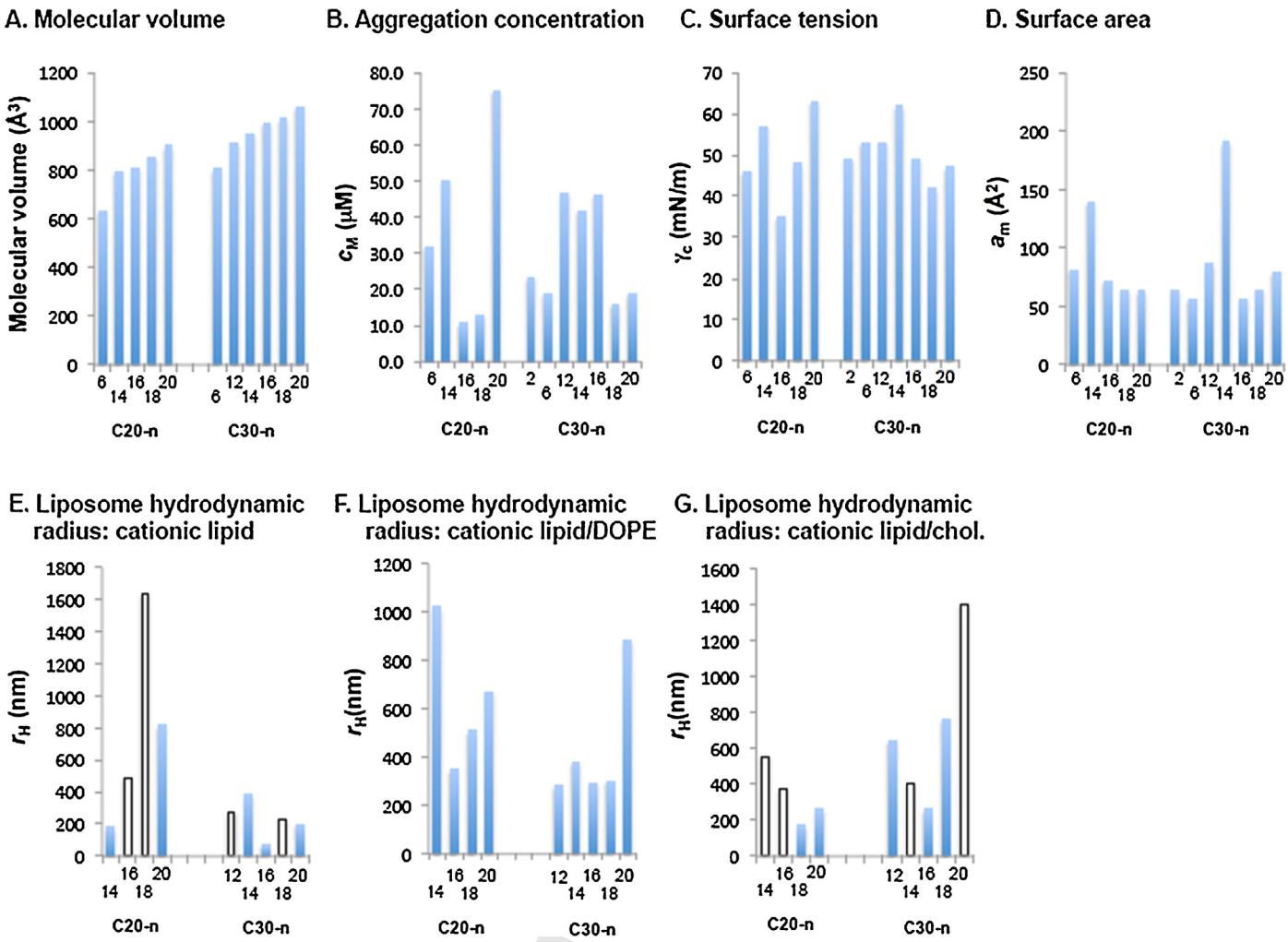

Fig. 9. Comparison of compound structure, surface data, and liposome size. The linear increase in molecular volume is not reflected in the physical and structural data obtained during characterization of the lipids. (A) Calculated molecular volume (Å^3). (B) Aggregation concentration c_M (μM). (C) Surface tension γ_c (mN/m). (D) Surface area a_m (Å^2). (E) Hydrodynamic radius r_H (nm) of liposomes composed of cationic lipids. (F) Hydrodynamic radius r_H (nm) of liposomes composed of cationic lipids with DOPE as a co-lipid. (G) Hydrodynamic radius r_H (nm) of liposomes composed of cationic lipids with cholesterol as a co-lipid. The open bars represent hydrodynamic radii derived from samples with a high polydispersity index (≥0.7) and thus, may not include a single population size.

polydispersity index (PdI) of lipoplexes in the C20-n and C30-n series ranged from of 0.2 to 1 (Table SI 2). PdI values greater than 0.7 indicated that multiple species or a broad distribution of sizes were present.

Lipoplexes formed by the reference lipid EPC were typically smaller without co-lipid and larger with either DOPE or cholesterol (Chol). EPC lipoplexes were mono-disperse for all three formulations. The lipoplexes formed by EPC were relatively small (d_H < 600 nm) at low or high N/P ratios, while some formulations, particularly involving molar ratios between 1.5 and 5, included large structures exceeding 2 μ (Table SI 2).

It is easy to anticipate a regular relationship between lipoplex size and liposome size or between lipoplex size and the ratio of cationic lipids to DNA. However, our observations with lipoplexes containing cationic C20-n or C30-n lipids resist the application of a simple structure–property relationship. Some lipoplexes were smaller than the liposomes (**C20-14** liposome d_h = 180 nm, **C20-14** lipoplex N/P 0.5 d_h = 170 nm, **C30-18** liposome d_h = 230 nm, **C30-18** lipoplexes N/P 10 d_h = 120 nm. Other lipoplexes were significantly larger (e.g. **C20-18** liposome, **C20-18**/DOPE N/P 1.5 lipoplex, Table SI 2). The large lipoplexes may arise from liposome fusion in the buffer solution, from electrostatic adhesion of neighboring liposomes or from lipoplex aggregation (Balbino et al., 2012; Kedika and Patri, 2011). Small lipoplex structures could result from the compaction of the plasmid DNA by the cationic lipids associated with the liposomes through electrostatic and hydrophobic forces. The electrostatic adhesion of several small neighboring lipoplexes gives rise to large lipoplex aggregates. Since a structure–property relationship for liposomes was missing (Table 2), a correlation between lipoplex activity (i.e., DNA delivery) and their structural properties was, similarly, not expected (Fig. 9).

4.7. Gel retardation assays of lipoplexes

A gel retardation assay was employed to study the binding interaction in the lipoplexes between the C20-n and C30-n liposomes and DNA. The assay revealed that, in general, DNA binding improved with increasing lipid ratio in the lipoplex formulations; typically, near complete retention was achieved at an N/P ratio of approximately 5.0:1 or 10:1 (Fig. SI 1).

Please cite this article in press as: Øpstad, C.L., et al., Novel cationic polyene glycol phospholipids as DNA transfer reagents—Lack of a structure–activity relationship due to uncontrolled self-assembling processes. Chem. Phys. Lipids (2014), http://dx.doi.org/10.1016/j.chemphyslip.2014.04.006

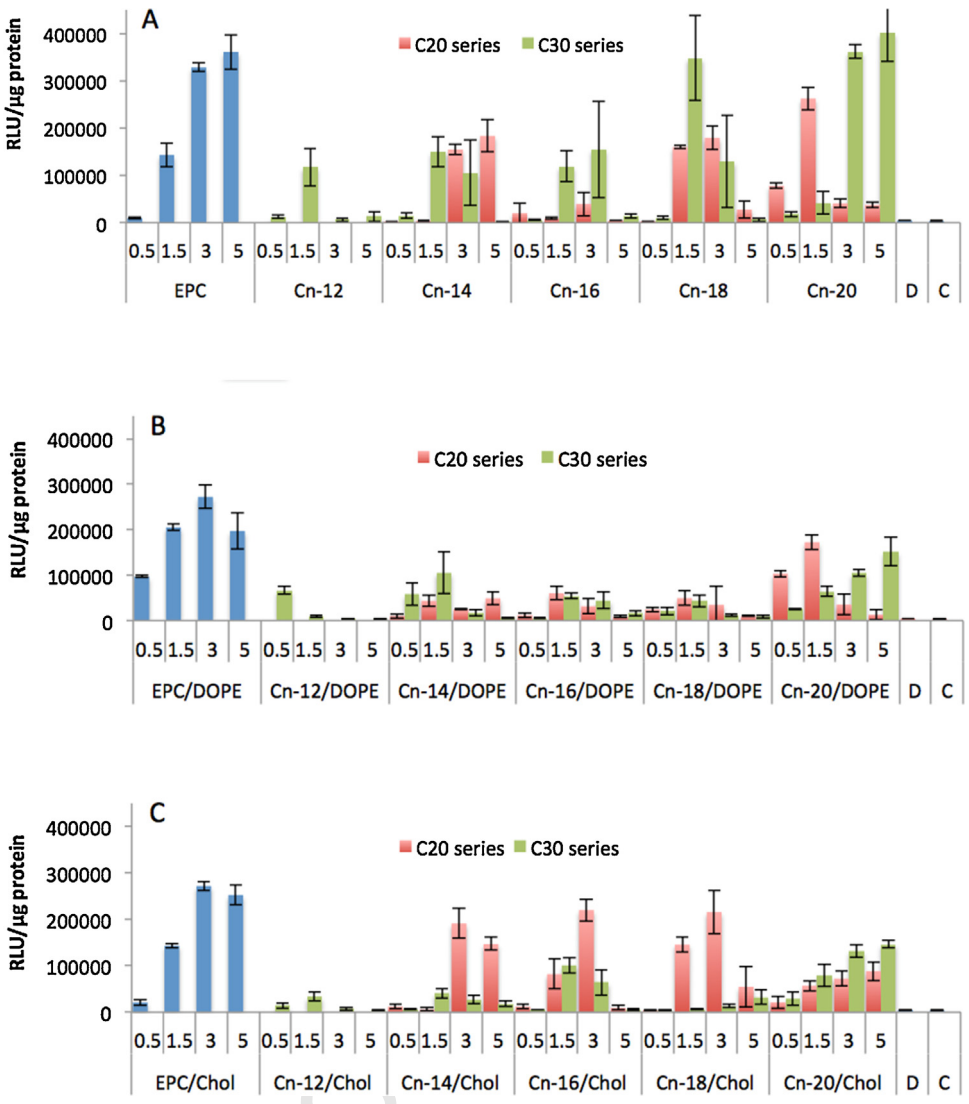

Fig. 10. Transfection efficiency to CHO-K1 cells for lipoplexes composed of EPC (blue bars, left), C20-n (red bars) or C30-n (green bars) at N/P ratios ranging from 0.5 to 5. Data are expressed in terms of the activity of the enzyme that was expressed by the transfected DNA (beta galactosidase) measured in relative light units (RLU) and normalized to the protein concentration of the transfected cell lysate (μg protein) collected 48 h after transfection. Negative controls included untreated cells ("C," blue bar, right) or cells treated with only DNA ("D," blue bar, right). (A) Transfection using lipoplexes formed from liposomes containing only cationic lipid C20-n or C30-n. (B) Transfection using lipoplexes formed from liposomes containing the cationic lipids plus DOPE as a co-lipid. (C) Transfection using lipoplexes formed from liposomes containing the cationic lipids plus Chol as a co-lipid. (For interpretation of the references to color in this figure legend, the reader is referred to the web version of the article.)

4.8. DNase I degradation assays of lipoplexes

A DNase I degradation assay verified the accessibility of the DNA in the lipoplexes to nucleases. DNA was partially protected from nuclease degradation in all lipoplex formulations at all charge ratios (Fig. SI 2). **C20-18** and **C20-20** based lipoplexes gave greater DNA protection, correlating with the better DNA binding observed in the gel retardation assays (Fig. SI 2). **C30-12** and **C30-20** lipoplexes appeared most protective. The C30-n/DOPE lipoplexes were equally protective for the DNA plasmid, whereas **C30-12**/Chol and **C30-20**/Chol were best in the C30-n/Chol formulations.

4.9. Transfection

Each liposome was formulated into lipoplexes by combination with DNA plasmids. The plasmid used for lipoplex formation contained a gene expression cassette including a gene for β-galactosidase to enable the detection of successful gene delivery to the nucleus of target cells resulting in the production of active enzyme. The enzyme activity was quantified as microgram of protein in the cell lysate of CHO-K1 cells. The values obtained with the C20-n and C30-n lipoplexes were generally significantly higher than those obtained from DOPE and Chol formulated lipoplexes. Remarkably, the lipid with the longest chains **C30-20** at N/P 3 and 5 functioned slightly better than EPC; the lipoplex of **C30-18** at N/P 1.5 was likewise outperforming EPC (Fig. 10). Lipoplexes formulated with DOPE and Chol showed significant transgene activity, though always lower than EPC. Gene expression was generally lower with DOPE than with Chol, especially in the case of several formulations of **C20-14**, **C20-16**, and **C20-18**. No trend appeared concerning performance for the C20-n and C30-n lipoplexes with

Please cite this article in press as: Øpstad, C.L., et al., Novel cationic polyene glycol phospholipids as DNA transfer reagents—Lack of a structure–activity relationship due to uncontrolled self-assembling processes. Chem. Phys. Lipids (2014), http://dx.doi.org/10.1016/j.chemphyslip.2014.04.006

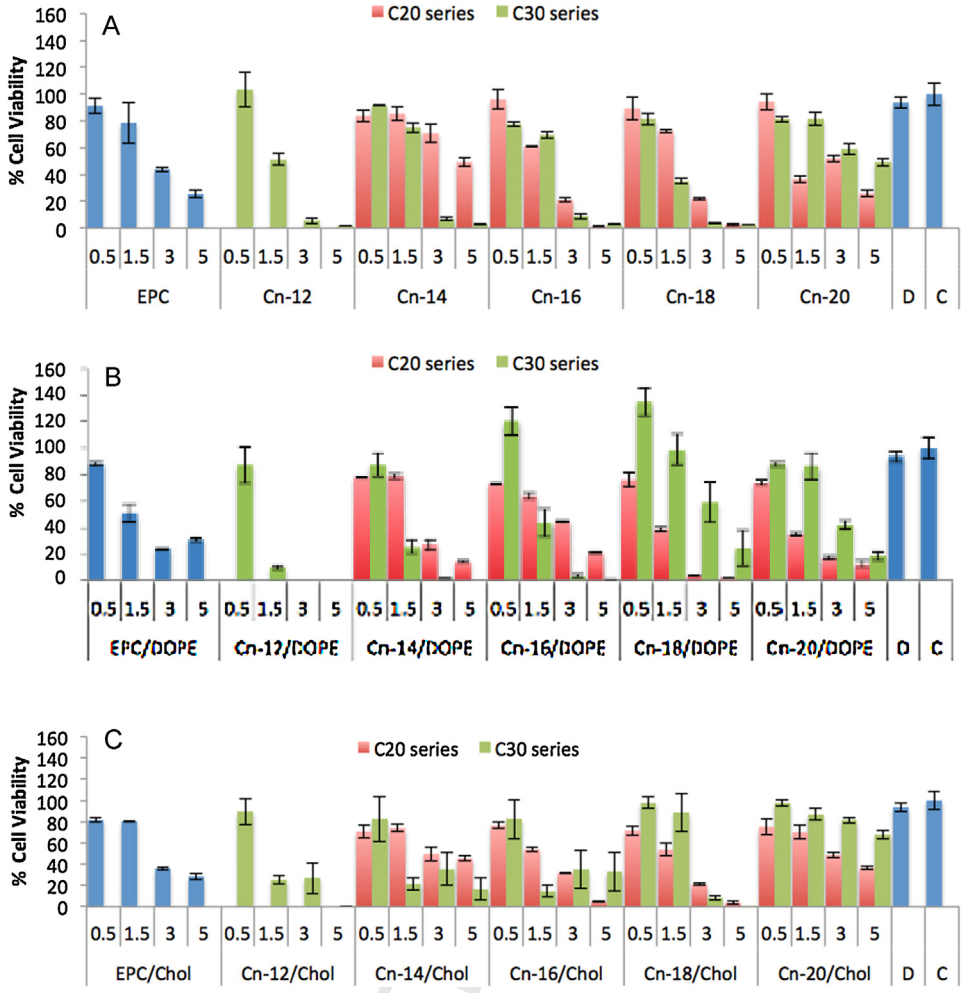

Fig. 11. Cell viability following transfection of CHO-K1 cells with lipoplexes composed of EPC (blue bars, left), C20-n (red bars) or C30-n (green bars) with N/P ratios ranging from 0.5 to 5. Data are expressed as percentage viability for CHO-K1 cells after 48 h compared to untreated cells ("C," blue bar, right) or cells treated with DNA alone ("D," blue bar, right). (A) Transfection using lipoplexes formed from liposomes containing only cationic lipid C20-n or C30-n. (B) Transfection using lipoplexes formed from liposomes containing cationic lipid plus DOPE as a co-lipid. (C) Transfection using lipoplexes formed from liposomes containing cationic lipid plus Chol as a co-lipid. (For interpretation of the references to color in this figure legend, the reader is referred to the web version of the article.)

respect to the variation of saturated chain length (Fig. 10). Recent studies contradictorily found improved gene delivery through increasing or decreasing unsaturation and reducing or elongating chain lengths (Jones et al., 2013; Liberska et al., 2009; Loizeau et al., 2013).

4.10. Transfection and lipoplex size

The importance of the lipoplex size for gene transfer has continuously been stressed. The most suitable lipoplex size has been attained either between 10 and 200 nm or 300 and 2000 nm (Almofti et al., 2003; Li and Szoka, 2007; Saha et al., 2012). Greater cellular association and uptake improved with larger lipoplexes in *in vitro* assays; endocytis with CHO-K1 cells was enhanced by increasing particle size to 2200 nm (Ross and Hui, 1999). Our data showed that lipoplex **C30-20** at N/P 5 (d_H = 600 nm) performed slightly better than small EPC lipoplex at N/P 5 (d_H = 280 nm, Fig. 10 and Table SI 2). Large **C30-20**/3 (d_H = 2080 nm) was likewise superior to small EPC/3 (d_H = 380 nm). **C30-18**/1.5 (d_H = 1770 nm) was more than double as effective in gene delivering than large EPC/1.5 lipoplex. Large **C20-20**/1.5 and **C20-18**/DOPE/1.5 transfected better than large EPC/1.5. The smallest lipoplexes, i.e. **C20-14**/0.5 (d_H = 170 nm) and EPC/0.5 (d_H = 150 nm) were both inactive in gene transfer. Thus lipoplex size is not a significant determinant for CHO-K1 cell transfection when using C20-n and C30-n based lipoplexes.

4.11. Cellular viability

Lipoplexes were generally well tolerated by CHO-K1 and relatively high transfection levels could be obtained, although enhanced transgene expression was accompanied by higher cytotoxicity (Fig. 11). Cell viability was, as expected, high with lipoplexes of low N/P ratios; increasing the N/P ratio decreased cell viability. Of interest, **C30-20** stood out among the new compounds in that it showed highest transfection efficiency, higher in fact than EPC in any formulation tested. At the same time, **C30-20** in the same formulations that provided high gene expression (N/P of 3 and 5 without co-lipid) lacked the characteristically high toxicity of those N/P ratios.

Please cite this article in press as: Øpstad, C.L., et al., Novel cationic polyene glycol phospholipids as DNA transfer reagents—Lack of a structure–activity relationship due to uncontrolled self-assembling processes. Chem. Phys. Lipids (2014), http://dx.doi.org/10.1016/j.chemphyslip.2014.04.006

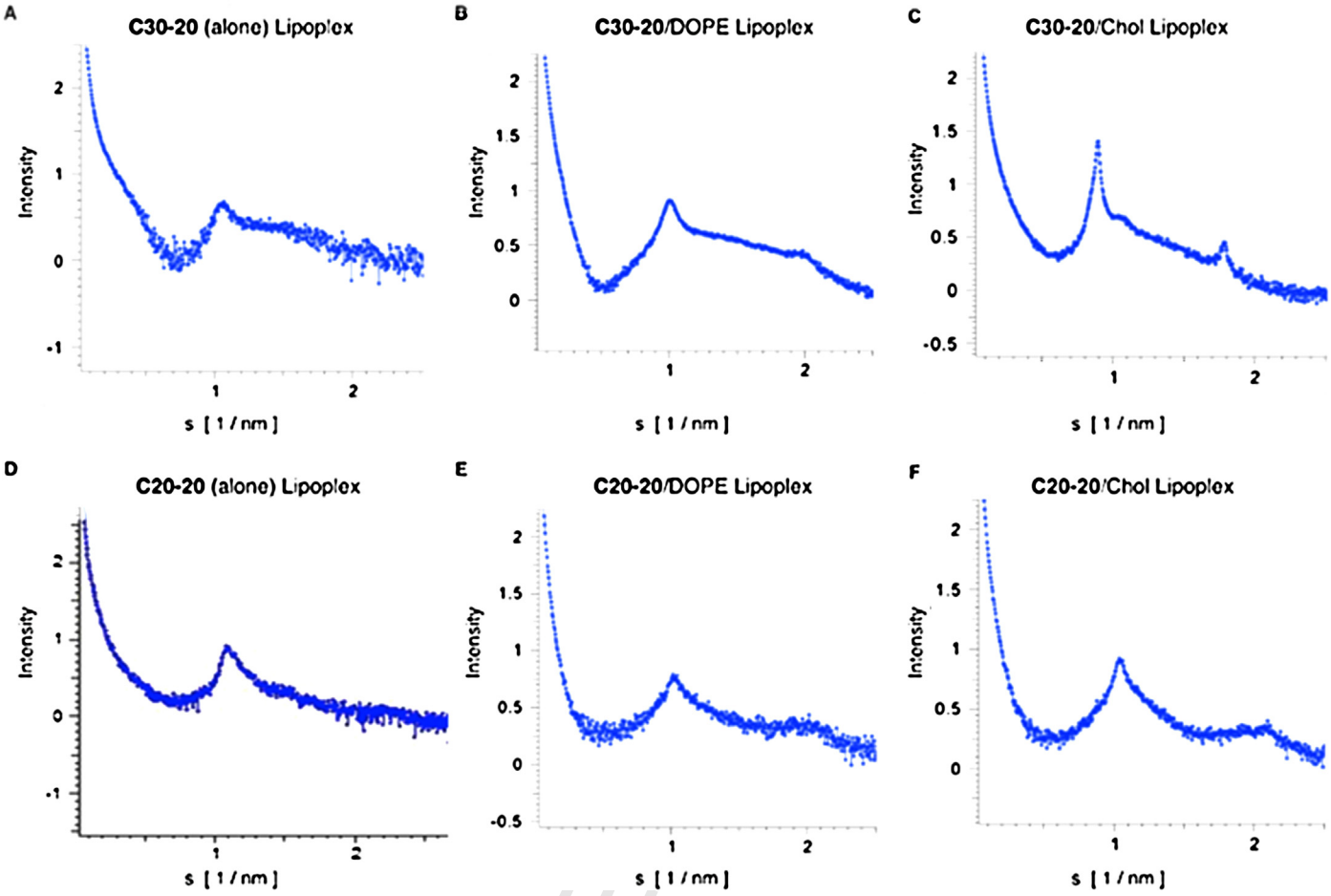

Fig. 12. SAXRD profile for **C30-20** and **C20-20** lipid/DNA lipoplex formulations without colipid (A and D), and with co-lipids DOPE (B and E) and cholesterol (C and F) an N/P molar charge ratio 1.5:1. Data are plotted as signal intensity (arbitrary units) as a function of the scattering vector.

Having completed a thorough analysis of physical and chemical characteristics of the novel lipids without obtaining a structure–property relationship, the further analysis of the bioactivity of lipoplexes did, similarly, not provide evidence of a structure–activity relationship (Figs. 10 and 11).

4.12. Small angle X-ray diffraction (SAXRD)

The intense X-rays provided by synchrotron sources have given rise to powerful tools for studying self-assembled nanostructures. One such technique is small angle X-ray scattering, which is useful for obtaining information on single particles. Additional information is available for those macromolecular systems whose structures are ordered, or partially ordered, because they can yield diffraction peaks that are superimposed on the SAXS spectrum. These peaks can be used to extract structural information. This is the situation for the lipid–DNA systems studied here and the data are logically designated as small angle X-ray diffraction (SAXRD). The scattering that constitutes SAXRD stems from single particle and inter-particle interference. Although the measurements were carried out using the SAXS experimental setup, it is the SAXRD part of the SAXS/SAXRD data that we make use of and which is analyzed here.

SAXRD data were measured for **C20-20** and **C30-20** liposomes and lipoplexes and those formulated with DOPE and cholesterol, all at an N/P ratio of 1.5. The presence of at least a single sharp peak expresses periodicity within the lipoplex membrane. The unimodal SAXS profile of the liposomes is associated with the absence of ordered arrangements. Similarly, the broad peaks of **C20-20** and **C30-20** lipoplexes are consistent with reduced bilayer order (Fig. 12), and, therefore, a precise value for the interlayer distance (δ) is difficult to obtain, although an approximate value may be extracted. The SAXRD profile of **C20-20**/DOPE and **C20-20**/Chol with their broad primary diffraction peaks and barely emergent secondary peaks are consistent with the evolution of periodicity. The secondary diffraction peak of lipoplex **C30-20**/DOPE (Fig. 12) is somewhat better resolved, reflecting a move to a more intervallic structure. The two narrow diffraction peaks of **C30-20**/Chol stem from the presence of ordered domains, most likely lamellar structures. The small shoulder near the intense SAXS-peak of **C30-20**/Chol is compatible with a diffraction signature from the DNA-strands in the lamellar segments, indicating an in-plane distance between the strands of $d_{DNA} \approx 59$ Å. The well-defined lamellar ordering of **C30-20**/Chol at 20 °C is still maintained when the temperature is raised to 55 °C; the small DNA peak became slightly more visible at higher temperature (Fig. SI 3).

The SAXRD profiles of **C20-20** and **C30-20** lipoplexes in Fig. 12 are most likely consistent with lamellar ordering with repetition distances given in Table 3. Comparison of the lipoplex profiles of these two rigid chain lipids with that of the lipoplex of EPC with its flexible chains (Fig. SI 4) is consistent with the bilayer being disrupted by the polyene chains. The effect of a disrupted bilayer on transfection efficiency is not clear. At an N/P ratio of 1.5, **C20-20** lipoplexes were least organized but were more effective than either **C20-20**/DOPE or

Please cite this article in press as: Øpstad, C.L., et al., Novel cationic polyene glycol phospholipids as DNA transfer reagents—Lack of a structure–activity relationship due to uncontrolled self-assembling processes. Chem. Phys. Lipids (2014), http://dx.doi.org/10.1016/j.chemphyslip.2014.04.006

Table 3
Microstructure and interlayer distance δ of the lipoplexes derived from SAXRD diffraction data (the corresponding liposomes did not exhibit diffraction).

Lipid formulation	Lipoplex (N/P = 1.5:1)	
	Profile	Distance δ (Å)
C30-20	Lamellar (most likely)	~59
C30-20/DOPE	Lamellar	63
C30-20/Chol	Lamellar	70
C20-20	Lamellar (most likely)	~58
C20-20/DOPE	Lamellar	~61
C20-20/Chol	Lamellar	~60

C20-20/Chol in DNA delivery (Fig. 10). In contrast, the DNA transfection efficiency of **C30-20** lipoplexes was low and similar to the more highly organized **C30-20**/DOPE or **C30-20**/Chol at N/P 1.5. But at a slightly higher N/P ratio of either 3 or 5, the transfection efficiency of **C30-20** was noticeably improved with all three formulations (Fig. 10). Thus, the adverse effect of the rigid chains on ordering does not predict transfection efficiency using the formulations tested here. Ultimately, destabilization of bilayers by rigid polyenes may prove to influence fusion and unpackaging of lipoplexes inside of cells.

4.13. Chain rigidity-flexibility, configuration, and transfection

Alkyl chain flexibility in phospholipid membranes accounts for molecular conformer changes accompanied by phase transitions from gel to fluid liquid crystalline (Mineva et al., 2013). Aggregation distorts as well the polyene chain of phospholipids, even though in a much more restricted manner (Foss et al., 2005a). The polyene chains in the C20-n and C30-n lipids are, therefore, considered rigid. At N/P 3 and 5 the achiral glycol lipid **C30-20** with an unsaturated rigid chain transfected cells to a comparable level as the glycerolipid enantiomer (*R*)-EPC with two flexible saturated chains.

5. Conclusion

A new class of cationic glycol phospholipids has been synthesized with chromophoric, rigid polyene chains and flexible alkyl chains. Essential property data such as surface tension γ, aggregate concentration c_M and the molecular area a_m could not be interconnected with the structure of the C20-n and C30-n compounds. When the homologous C20-n and C30-n amphiphiles came in contact with water, a heterologous behavior was observed caused by unpredictable assembling of the molecules to aggregates and liposomes. Neither liposome nor lipoplex dimensions were defined by chain lengths. The combination of a C30:9 chain with a C20:0 alkyl chain showed the best *in vitro* DNA transfection. However, this result could not be linked to other parameters. Formulations employing co-lipids DOPE or cholesterol revealed no trend in transfection with the lengths of saturated and polyunsaturated chains.

Lipoplexes of achiral **C30-20** with a rigid polyene chain and a flexible saturated chain behaved in transfecting CHO-K1 cells comparable to reference (*R*)-EPC with two flexible saturated chains. Consequently, avoiding chirality and introducing a rigid polyene chain had no obvious effect within our reference frame.

The periodicity in the bilayers of EPC with saturated chains is disturbed in compounds with a rigid polyene chain as established by SAXRD. However, the presence or absence of an ordered microstructure had no influence on transfections when comparing **C30-20** with EPC.

Although selected members of the new lipids with low cytotoxicity offer promising gene delivery performance providing a basis for further investigating a structure–activity connection could not be established.

As stated previously, the magnitude of biological and chemical variables have so far prevented establishing an unambiguous structure–activity connection (Koynova and Tenchov, 2010; Zhi et al., 2010, 2013). This report has demonstrated that the reason for the lack of regularities between structural and physical data, and transfection of the polyene gene carriers is caused by their uncontrollable molecular associations. This finding supports a complementing conclusion articulated in a recent investigation on lipid packing and transfection (Moghaddam et al., 2011).

A straightforward structure–activity correlation may only be established when the outcome of the self-assembly processes, i.e. size, fine structure, morphology, DNA compacting, could be controlled, e.g. by relying on liposomes and lipoplexes of predefined shape and size (Svenson, 2004). The preparation of liposomes with defined size and shape will be the topic of a forthcoming communication.

Conflict of Interest

The authors declare that there are no conflicts of interest.

Acknowledgements

We thank Dr. Hansgeorg Ernst, BASF SE, Ludwigshafen (Germany) for a generous gift of C30-ester, and Dr. Susana V. Gonzales (NTNU) and Dr. Zhihua Yang (Stevens) for performing mass spectrometric determinations. Synchrotron beam time was granted by the European Synchrotron Radiation Facility, Grenoble, France, using the facilities of the BIOSAXS beamline (BM29). We are grateful to Adam Round and Christoph Mueller-Dieckmann for technical assistance in setting up the experiments for the SAXS/SAXRD data collection. AZ thanks the Higher Education Commission of Pakistan for a scholarship. This work was made possible by a grant from the Qatar National Research Fund under the National Priorities Research Program, award NPRP08-705-3-144 (LPI: M. Pungente). Its contents are solely the responsibility of the authors and do not necessarily represent the official views of the Qatar National Research Fund.

Appendix A. Supplementary data

Supplementary data associated with this article can be found, in the online version, at http://dx.doi.org/10.1016/j.chemphyslip.2014.04.006.

References

Adami, R.C., Seth, S., Harvie, P., Johns, R., Fam, R., Fosnaugh, K., Zhu, T.Y., Farber, K., McCutcheon, M., Goodman, T.T., Liu, Y., Chen, Y., Kwang, E., Templin, M.V., Severson, G., Brown, T., Vaish, N., Chen, F., Charmley, P., Polisky, B., Houston, M.E., 2011. An amino acid-based amphoteric liposomal delivery system for systemic administration of siRNA. Mol. Ther. 19, 1141–1151.
Almofti, M.R., Harashima, H., Shinohara, Y., Almofti, A., Li, W.H., Kiwada, H., 2003. Lipoplex size determines lipofection efficiency with or without serum. Mol. Membr. Biol. 20, 35–43.
Antipina, M.N., Schulze, I., Heinze, M., Dobner, B., Langner, A., Brezesinski, G., 2009. Physical–chemical properties and transfection activity of cationic lipid/DNA complexes. ChemPhysChem 10, 2471–2479.
Balbino, T.A., Gasperini, A.A.M., Oliveira, C.L.P., Azzoni, A.R., Cavalcanti, L.P., de La Torre, L.G., 2012. Correlation of the physicochemical and structural properties of pDNA/cationic liposome complexes with their in vitro transfection. Langmuir 28, 11535–11545.
Bergelson, L.D., 1970. Diol lipids. Prog. Chem. Fats Lipids 10, 241–286.
Breukers, S., Øpstad, C.L., Sliwka, H.R., Partali, V., 2009. Hydrophilic carotenoids: surface properties and aggregation behavior of the potassium salt of the highly unsaturated diacid norbixin. Helv. Chim. Acta 92, 1741–1747.
Byun, H.S., Bittman, R., 1996. Efficient stereospecific synthesis of diamide analogs of phosphatidylcholine starting from 1-(4′-methoxyphenyl)-sn-glycerol. J. Org. Chem. 61, 8706–8708.
Chang, C.D., Siegel, C., Lee, E., Harris, D.J., 1997. Intermolecular acyl group exchange between cationic lipid and co-lipid of cationic lipid-based gene transfer agents. Abstr. Pap. 214 Nat. Meeting, Am. Chem. Soc., 19-ANYL.
Chu, Y., Masoud, M., Gebeyehu, G., 2009. US Patent 7,479,573. Transfection Reagents, Invitrogen, USA.
Coste, J., Frérot, E., Jouin, P., 1994. Coupling N-methylated amino-acids using pybrop and pyclop halogenophosphonium salts – mechanism and fields of application. J. Org. Chem. 59, 2437–2446.
Dabkowska, A.P., Barlow, D.J., Hughes, A.V., Campbell, R.A., Quinn, P.J., Lawrence, M.J., 2012. The effect of neutral helper lipids on the structure of cationic lipid monolayers. J. R. Soc. Interface 9, 548–561.
Felgner, P.L., Gadek, T.R., Holm, M., Roman, R., Chan, H.W., Wenz, M., Northrop, J.P., Ringold, G.M., Danielsen, M., 1987. Lipofection – a highly efficient, lipid-mediated DNA-transfection procedure. Proc. Natl. Acad. Sci. U.S.A. 84, 7413–7417.
Floch, V., Loisel, S., Guenin, E., Hervé, A.C., Clément, J.C., Yaouanc, J.J., des Abbayes, H., Férec, C., 2000. Cation substitution in cationic phosphonolipids: a new concept to improve transfection activity and decrease cellular toxicity. J. Med. Chem. 43, 4617–4628.
Foss, B.J., Nalum Naess, S., Sliwka, H.R., Partali, V., 2003. Stable and highly water-dispersible, highly unsaturated carotenoid phospholipids – surface properties and aggregate size. Angew. Chem. Int. Ed. 42, 5237–5240.
Foss, B.J., Sliwka, H.R., Partali, V., Cardounel, A.J., Zweier, J.L., Lockwood, S.F., 2004. Direct superoxide anion scavenging by a highly water-dispersible carotenoid phospholipid evaluated by electron paramagnetic resonance (EPR) spectroscopy. Bioorg. Med. Chem. Lett. 14, 2807–2812.
Foss, B.J., Sliwka, H.R., Partali, V., Köpsel, C., Mayer, B., Martin, H.D., Zsila, F., Bikadi, Z., Simonyi, M., 2005a. Optically active oligomer units in aggregates of a highly unsaturated, optically inactive carotenoid phospholipid. Chem. Eur. J. 11, 4103–4108.
Foss, B.J., Sliwka, H.R., Partali, V., Naess, S.N., Elgsaeter, A., Melø, T.B., Naqvi, K.R., 2005b. Hydrophilic carotenoids: surface properties and aggregation behavior of a highly unsaturated carotenoid lysophospholipid. Chem. Phys. Lipids 134, 85–96.
Foss, B.J., Sliwka, H.R., Partali, V., Naess, S.N., Elgsaeter, A., Melø, T.B., Naqvi, K.R., O'Malley, S., Lockwood, S.F., 2005c. Hydrophilic carotenoids: surface properties and aqueous aggregation of a rigid, long-chain, highly unsaturated dianionic bolaamphiphile with a carotenoid spacer. Chem. Phys. Lipids 135, 157–167.
Ginn, S.L., Alexander, I.E., Edelstein, M.L., Abedi, M.R., Wixon, J., 2013. Gene therapy clinical trials worldwide to 2012 – an update. J. Gene Med. 15, 65–77.
Goldberg, M.S., (Ph.D. Thesis) 2008. Screening, Synthesis, and Applications of "Lipidoids", A Novel Class of Molecules Developed for the Delivery of RANi Therapeutics, Chemistry. Massachusets Institute of Technology, Boston, pp. 35.
Hirsch-Lerner, D., Zhang, M., Eliyahu, H., Ferrari, M.E., Wheeler, C.J., Barenholz, Y., 2005. Effect of "helper lipid" on lipoplex electrostatics. Biochim. Biophys. Acta 1714, 71–84.
Horn, D., Rieger, J., 2001. Organic nanoparticles in the aqueous phase – theory, experiment, and use. Angew. Chem. Int. Ed. 40, 4331–4361.
Ivanova, E.A., Maslow, M.A., Kabilova, T.O., Puchkov, P.A., Alekseeva, A.S., Boldyrev, I.A., Vlassov, V.V., Serebrennikova, G.A., Morozova, N.G., Zenkova, M.A., 2013. Structure–transfection acitivity relationships in a series of novel cationic lipids with heterocycic head-groups. Org. Biomol. Chem. 11, 7164–7178.
Jones, C.H., Chen, C.K., Ravikrishnan, A., Rane, S., Pfeifer, B.A., 2013. Overcoming nonviral gene delivery barriers: perspective and future. Mol. Pharm. 10, 4082–4098.
Kedika, B., Patri, S.V., 2011. Design, synthesis, and in vitro transfection biology of novel tocopherol based monocationic lipids: a structure–activity investigation. J. Med. Chem. 54, 548–561.
Konarev, P.V., Volkov, V.V., Sokolova, A.V., Koch, M.H.J., Svergun, D.I., 2003. PRIMUS: a Windows PC-based system for small-angle scattering data analysis. J. Appl. Crystallogr. 36, 1277–1282.
Koynova, R., 2010. Analysis of lipoplex structure and lipid phase changes. Methods Mol. Biol. 606, 399–423.
Koynova, R., Tenchov, B., 2009. Cationic phospholipids: structure–transfection activity relationships. Soft Matter 5, 3187–3200.
Koynova, R., Tenchov, B., 2010. Cationic lipids: molecular structure/transfection activity relationships and interactions with biomembranes. Top. Curr. Chem. 296, 51–93.
Koynova, R., Tenchov, B., Wang, L., MacDonald, R.C., 2009. Hydrophobic moiety of cationic lipids strongly modulates their transfection activity. Mol. Pharm. 6, 951–958.
Larsen, E., Abendroth, J., Partali, V., Schulz, B., Sliwka, H.R., Quartey, E.G.K., 1998. Combination of vitamin E with a carotenoid: alpha-tocopherol and trolox linked to beta-apo-8′-carotenoic acid. Chem. Eur. J. 4, 113–117.
Li, W.J., Szoka, F.C., 2007. Lipid-based nanoparticles for nucleic acid delivery. Pharm. Res. 24, 438–449.
Liberska, A., Unciti-Broceta, A., Bradley, M., 2009. Very long-chain fatty tails for enhanced transfection. Org. Biomol. Chem. 7, 61–68.
Loizeau, D., Le Gall, T., Mahfoudhi, S., Berchel, M., Maroto, A., Yaouanc, J.J., Jaffres, P.A., Lehn, P., Deschamps, L., Montier, T., Giamarchi, P., 2013. Physicochemical properties of cationic lipophosphoramidates with an arsonium head group and various lipid chains: a structure–activity approach. Biophys. Chem. 171, 46–53.
Mangroo, D., Gerber, G.E., 1988. Phospholipid synthesis – effects of solvents and catalysts on acylation. Chem. Phys. Lipids 48, 99–108.
Mathematica, 2010. Mathematica Version 8.0. Wolfram Research Inc., University of Illinois Press, Champaign, IL.
Merkel, O.M., Mintzer, M.A., Librizzi, D., Samsonova, O., Dicke, T., Sproat, B., Garn, H., Barth, P.J., Simanek, E.E., Kissel, T., 2010. Triazine dendrimers as nonviral vectors for in vitro and in vivo RNAi: the effects of peripheral groups and core structure on biological activity. Mol. Pharm. 7, 969–983.
Mineva, T., Krishnamurty, S., Salahub, D.R., Goursot, A., 2013. Temperature dependence of the molecular conformations of dilauroyl phosphatidylcholine: a density functional study. Int. J. Quantum Chem. 113, 631–636.
Moghaddam, B., McNeil, S.E., Zheng, Q., Mohammed, A.R., Perie, Y., 2011. Exploring the correlation between lipid packing in lipoplexes and their transfection efficacy. Pharmaceutics 3, 846–848.
Niculescu-Duvaz, D., Heyes, J., Springer, C.J., 2003. Structure–activity relationship in cationic lipid mediated gene transfection. Curr. Med. Chem. 10, 1233–1261.
Øpstad, C.L., Sliwka, H.R., Partali, V., Elgsaeter, A., Leopold, P.L., Jubeli, E., Khalique, N.A., Raju, L., Pungente, M.D., 2013. Synthesis, self-assembling and gene delivery potential of a novel highly unsaturated, conjugated cationic phospholipid. Chem. Phys. Lipids 170–171, 65–73.
Popplewell, L.J., Abu-Dayya, A., Khanna, T., Flinterman, M., Khalique, N.A., Raju, L., Øpstad, C.L., Sliwka, H.R., Partali, V., Dickson, G., Pungente, M.D., 2012. Novel cationic carotenoid lipids as delivery vectors of antisense oligonucleotides for exon skipping in Duchenne muscular dystrophy. Molecules 17, 1138–1148.
Pozzi, D., Marchini, C., Cardarelli, F., Amenitsch, H., Garulli, C., Bifone, A., Caracciolo, G., 2012. Transfection efficiency boost of cholesterol-containing lipoplexes. Biochim. Biophys. Acta 1818, 2335–2343.
Predvoditilev, D.A., Suvorkin, S.V., Nifant'ev, E.E., 2001. New approach to the synthesis of phosphamide models of cationic phosphatidyl cholines. Russ. J. Gen. Chem. 71, 873–880.
Rosenzweig, H.S., Rakhmanova, V.A., McIntosh, T.J., MacDonald, R.C., 2000. O-alkyl dioleoylphosphatidylcholinium compounds: the effect of varying alkyl chain length on their physical properties and in vitro DNA transfection activity. Bioconjug. Chem. 11, 306–313.
Ross, P.C., Hui, S.W., 1999. Lipoplex size is a major determinant of in vitro lipofection efficiency. Gene Ther. 6, 651–659.

Please cite this article in press as: Øpstad, C.L., et al., Novel cationic polyene glycol phospholipids as DNA transfer reagents—Lack of a structure–activity relationship due to uncontrolled self-assembling processes. Chem. Phys. Lipids (2014), http://dx.doi.org/10.1016/j.chemphyslip.2014.04.006

Ryhänen, S., 2006. Biophysical Studies on Cationic Liposomes. University of Helsinki, Finland, pp. 55.
Q7 Saha, K., Kim, S.T., Yan, B., Miranda, O.R., Alfonso, F.S., Shlosman, D., Rotello, V.M., 2012. Surface functionality of nanoparticles determines the cellular uptake mechanisms in mammalian cells. Small.
Scheule, R.K., Bagley, R.G., Eastman, S.J., Cheng, S.H., Marshall, J., Yew, N.S., Harris, D.J., Lee, E.R., Siegel, C.S., Chang, C.D., Hubbard, C.S., 1998. Cationic Amphiphile/DNA Complexes. Genzyme Corporation, USA.
Shinoda, K., 1963. Colloidal Surfactants. Some Physial Chemical Properties. Academic Press, New York.
Skrylev, L.D., Streltsova, E.A., Skryleva, T.L., 2000. Adsorption-micellar energy ratio as criterion for predicting surfactant performance. Russ. J. Appl. Chem. 73, 1364–1367.
Sliwka, H.R., 1997. Selenium carotenoids 3: first synthesis of optically active carotenoid phosphates. Acta Chem. Scand. 51, 345–347.
Sliwka, H.R., 1999. Conformation and circular dichroism of beta,beta-carotene derivatives with nitrogen-, sulfur-, and selenium-containing substituents. Helv. Chim. Acta 82, 161–169.
Sliwka, H.R., Partali, V., Lockwood, S.F., 2010. Hydrophilic carotenoids: carotenoid aggregates. In: Landrum, J.T. (Ed.), Carotenoids – Physical, Chemical and Biological Funtions and Properties. CRC Press, Boca Raton, p. 47.
Svenson, S., 2004. Controlling surfactant self-assembly. Curr. Opin. Colloid Interface Sci. 9, 201–212.
Wang, C., Berg, C.J., Hsu, C.C., Merrill, B.A., Tauber, M.J., 2012. Characterization of carotenoid aggregates by steady-state optical spectroscopy. J. Phys. Chem. B 116, 10617–10630.
Yoshimura, T., Chiba, N., Matsuoka, K., 2012. Supra-long chain surfactants with double or triple quaternary ammonium headgroups. J. Colloid Interface Sci. 374, 157–163.
Zhi, D., Zhang, S., Cui, S., Zhao, Y., Wang, Y., Zhao, D., 2013. Headgroup evolution of cationic lipids for gene delivery. Bioconjug. Chem. 24, 487–519.
Zhi, D.F., Zhang, S.B., Wang, B., Zhao, Y.N., Yang, B.L., Yu, S.J., 2010. Transfection efficiency of cationic lipids with different hydrophobic domains in gene delivery. Bioconjug. Chem. 21, 563–577.

Please cite this article in press as: Øpstad, C.L., et al., Novel cationic polyene glycol phospholipids as DNA transfer reagents—Lack of a structure–activity relationship due to uncontrolled self-assembling processes. Chem. Phys. Lipids (2014), http://dx.doi.org/10.1016/j.chemphyslip.2014.04.006